

DAMPED ARM RESTRAINT
FOR TREMOR PATIENTS

by

Susan Russell Stapleton

SUBMITTED IN PARTIAL FULFILLMENT
OF THE REQUIREMENTS FOR THE
DEGREE OF
BACHELOR OF SCIENCE
IN COURSE 2-A
THROUGH THE DEPARTMENT OF
MECHANICAL ENGINEERING

at the

MASSACHUSETTS INSTITUTE OF TECHNOLOGY

May 1982

Signature of Author _____

Department of Mechanical Engineering
May 14, 1982

Certified by _____

Michael J. Rosen
Thesis Supervisor

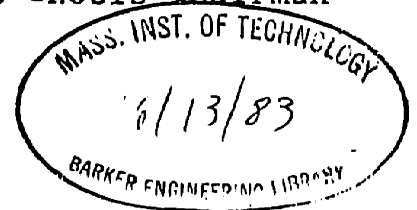
Accepted by _____

Eng. Department Thesis Chairman

MASSACHUSETTS INSTITUTE
OF TECHNOLOGY

JUN 24 1982

LIBRARIES



DAMPED ARM RESTRAINT
FOR TREMOR PATIENTS

by

Susan Russell Stapleton

Submitted to the Department of Mechanical Engineering
on May 14, 1982 in partial fulfillment of the
requirements for the Degree of Bachelor of Science in
Course 2-A.

ABSTRACT

A viscously damped arm restraint as a mechanical loading method for the suppression of abnormal intention tremor in the upper extremity was analyzed to: 1) determine deviations from ideal omni-directional damper behavior; 2) test the feasibility of independent restraint of each arm restraint.

The design of a constrained, compliant arm restraint was proposed and a mathematical analysis of a model of the system was conducted using normalized equations.

The best damping characteristics were found with a restraint with equal length links, a reach of about twice that of the arm, and variable continuous rotational dampers which could be adjusted for each system configuration.

Thesis Supervisor: Dr. Michael J. Rosen

Title: Principal Research Scientist,
Department of Mechanical Engineering

TABLE OF CONTENTS

	<u>Page</u>
TITLE PAGE	1
ABSTRACT	2
TABLE OF CONTENTS.	3
CHAPTER 1 - INTRODUCTION	4
1-1 Statement of Thesis.	4
1-2 Classification of Tremor	4
1-3 Etiology of Tremor	5
1-4 Methods of Tremor Suppression.	5
CHAPTER 2 - APPARATUS.	7
2-1 Design Alternatives.	7
2-2 Tentative Description of Apparatus	8
CHAPTER 3 - ANALYSIS	11
3-1 Objective of Analysis.	11
3-2 Method of Analysis	11
3-3 Mathematical Analysis.	12
3-4 Normalization of Equations	19
3-5 Summary of Normalized Equations.	25
CHAPTER 4 - RESULTS.	26
4-1 Introduction	26
4-2 Verification of Results.	26
4-2-1 Special Case	26
4-2-2 General Case	30
4-3 Interpretation of Results.	32
4-3-1 Reading of Plots	32
4-3-2 Ideal Damping.	32
4-3-3 Effects of Varying parameters.	37
CHAPTER 5 - SUMMARY AND CONCLUSION	45
APPENDIX A- COMPUTER PROGRAM LISTINGS.	46
APPENDIX B- PLOTS OF NORMALIZED FORCE COMPONENTS	52

Chapter 1-Introduction

1-1 Statement of Thesis

The objective of this thesis is the analysis of a viscously damped arm restraint as a mechanical loading method for the suppression of intention tremor in the upper extremity. Particularly, the goal is to: 1) determine deviations from ideal omni-directional damper behavior; 2) test the feasibility of independent restraint of each arm joint.

1-2 Classification of Tremor

Tremor is most generally defined as a series of rhythmic, involuntary movements caused by the contraction of opposing muscle groups. (1) Normal physiological tremor is present in all individuals to some extent, but is of such high frequency and low amplitude that it does not usually interfere with ordinary activity. Pathological tremor, however, can be sufficiently severe to impair the individual's ability to perform normal tasks.

Tremors can be roughly classified as "resting tremors", "postural tremors", or "action tremors". Resting tremors, such as that seen in Parkinson's disease, occur when the muscles are completely at rest. Postural tremors involve the muscle groups concerned with maintaining support of the body. Action tremors occur during the execution of motor tasks. (1)

This thesis deals with a means of suppressing intention tremor, a type of action tremor involving purposeful, "intended" movements of a limb. Intention tremor, hereafter to

be called simply "tremor", is characterized by low frequency, high amplitude oscillations,(8) which are accentuated by direction changes of the affected limb.(1) The oscillations can be so severe that they completely obscure the intended movement, making actions which require any degree of precision impossible. (8)

1-3 Etiology of Tremor

Tremor usually is a result of neurological damage or disease. Damage to the spino-cerebellar and midbrain centers associated with head injury, stroke, or tumors, as well as lesions from multiple sclerosis on neurological pathways, often results in tremor. It is also seen in individuals with Friedreich's Ataxia, Cerebral Palsy, chronic alcohol intoxication, metabolic poisoning, and other degenerative diseases. (7) Although exact figures are not available, it has been estimated that about 800,000 people in the United States alone are disabled by tremor. (8) Clearly, there is a need to determine an effective and safe method of tremor suppression.

1-4 Methods of Tremor Suppression

Suppression of tremor by surgical methods and drugs have been attempted, but have shown generally poor and inconsistent results. Thalamic surgery, surgical ablation of parts of the thalamus, was reported by Cooper to be completely successful, but those results were contradicted by van Manen, who reported complete failure for tremors of several etiologies. (8) Considering the risks involved in surgery, such a

method does not appear to be a viable alternative. Treatment with drugs effective on Parkinsonian tremors, such as L-dopa and amantadine, are not effective on intention tremor. (4) Administration of propranolol or ethanol do attenuate tremor, but the effect is transient. (7,11) The possible side effects of drug treatment must also be considered.

External mechanical methods have also been examined for their effectiveness in the reduction of tremor. Chase et al was able to successfully reduce the magnitude of the oscillations by cooling the muscles involved in the tremor. Chase also investigated the effects of applying a constant force against the tremor, however, he found that although the tremor was reduced on extension, the force increased the amplitude of the tremor on flexion. Morgan, Hewer, and Cooper noted appreciable reduction of tremor when upper extremity tremors were mechanically loaded by attaching weights to the affected limbs. (5) Rosen et al has demonstrated a significant decrease in tremor with maintained accuracy in tracking tasks, by applying viscous damping to the affected limbs through a mechanical damping device. (8)

Mechanical loading of the affected limbs appears to be a promising method for the suppression of intention tremors, especially considering the low level of safety risk. This thesis concentrates entirely upon mechanical loading of the upper extremity through a viscously damped arm restraint. This work represents a practical application of an approach to tremor management which has for the most part been confined to laboratory experiments.

Chapter 2-Apparatus

2-1 Design Alternatives

An apparatus, which would provide tremor suppression and be usable for such tasks as writing, eating, or other precision arm movements, would have great clinical value. A compliant restraint, which would suppress tremor without impeding arm movement, is a viable solution to this problem. One type of compliant restraint which has been investigated is a device specific interface, such as the damped joystick for use with a communication device designed at the MIT Rehabilitation Engineering Center (9,10), or the writing machine invented by James Fee, Jr. (2). A second type of compliant restraint is a wearable orthosis, which would be portable and useful in many applications. Although this is perhaps the optimal alternative, very little study has been done on the subject.

Another such device is a fixed base compliant restraint, which would act as a general purpose arm restraint within a defined work-space, limited in area by either the size of the apparatus or the length of the arm. This would provide two degrees of freedom, constrained by the anatomical characteristics of the human elbow, the location of the user's shoulder with respect to the base of the restraint, and the location of the restraint base itself. This thesis proposes a tentative design of such an apparatus, and considers its practicality in terms of the size and power requirements.

2-2 Tentative Description of Apparatus

One alternative design of the apparatus is based on a commercially available ball bearing feeder. The feeder, designed to attach to the arm of a wheelchair, consists of two links, each inserted in a swivel post, with an arm support at the terminal and pivot stops at the swivel posts may be adjusted to limit the range of movement.(6)

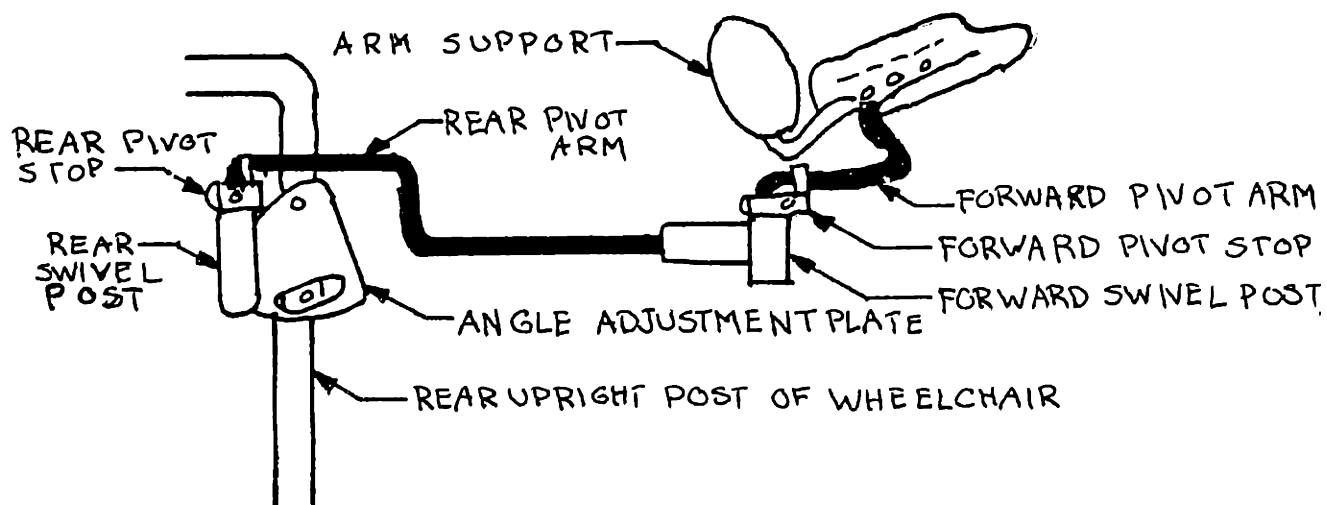


FIGURE 2-1
BALL BEARING FEEDER

The analysis of the device should determine if the feeder is sufficient as a basis for the apparatus, or if the restraint must be built in its entirety. If the feeder is sufficient as a viscously damped arm restraint by preloading the bearings to minimize play at the joints, and attaching continuous rotational dampers to the base of the pivot arms at the swivel

posts , as shown in Figure 2-2.

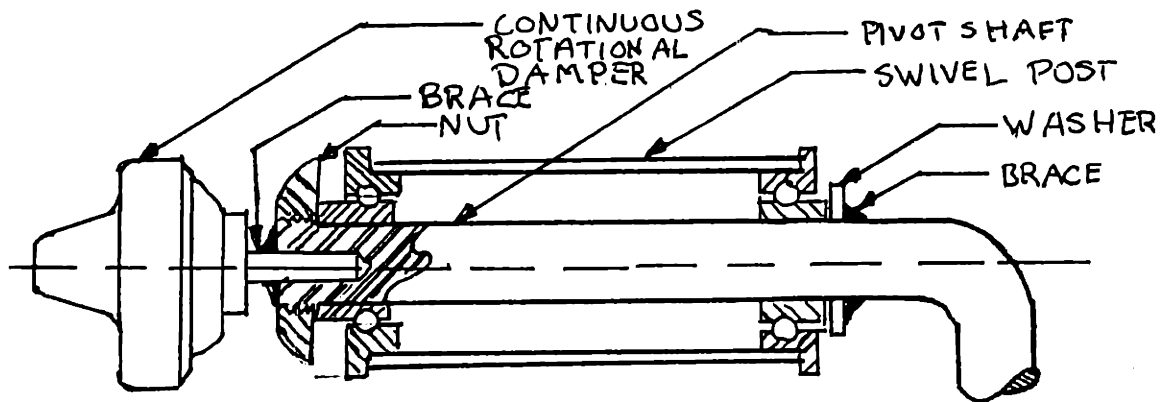


FIGURE 2-2
PROPOSED MODIFICATIONS OF BALL BEARING FEEDER

A velocity applied at the terminal point of the orthosis by the movement of individual's arm produces torques at the joints of the orthosis, and, consequently, a resistive force at the terminal point. Since the resistive force is proportional to the applied velocity, the dampers act as a mechanical filter, analogous to an RC filter, where only low frequency movements are passed. Thus, the high frequency, tremor-induced movements are filtered out.

For the purpose of this thesis, ideal restraint is defined as that which would provide omnidirectional damping at every point in the work-space, and independent restraint of each arm joint, since tremor could originate at either or both joints. For the analytical calculations, the ability of humans to produce the desired position and velocity trajectory is being assumed, and the resistive force is being computed from that. However, it must be considered that an

orthosis requiring large differences between the direction of the velocity and the force would be difficult to use.

Chapter 3-Analysis

3-1 Objective of Analysis

The objective of this analysis is to determine to what extent the arm restraint acts as an ideal omni-directional damper, and if independent restraint of human joints can be achieved.

The first step in this analysis is to determine the resistive force at the terminal point of the restraint, in response to a controlled velocity applied through that point. This can be accomplished by realizing that a velocity through the terminal point determines angular velocities through the orthosis joints, and those velocities, acting through rotational dampers, produce joint-torques which determine the resistive force at the terminal point.

3-2 Method of Analysis

The orthosis is attached to the wheelchair, at some distance away from the shoulder, and to the patient's arm, near the wrist. The orthosis can rotate at the point where it is attached to the wheelchair, and at a hinged joint, roughly corresponding to the human elbow. The patient can also rotate his arm about the shoulder and elbow. All movement is constrained to a plane perpendicular to the vertical axis of the body. Another constraint is put on the system since the elbow can not extend beyond an angle of 180° .

Thus, the system can be modeled as a four-bar linkage with five joints, and two degrees of freedom. Ground is defined along a line in the plane corresponding to the back of the wheelchair.

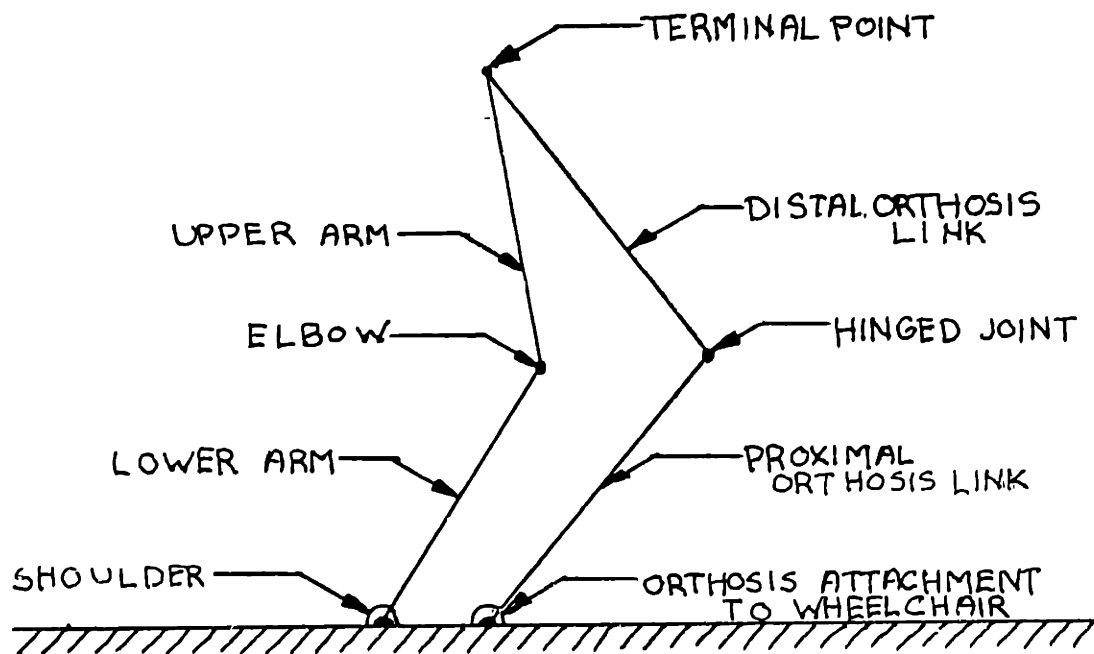


FIGURE 3-1
MODEL OF APPARATUS

Using cartesian coordinates, basic trigonometric identities, and the law of cosines, the angles at the orthosis joints can be determined. It is being assumed that the orthosis is essentially massless.

3-3 Mathematical-Analysis

Let:

l = the distance between the shoulder and the orthosis attachment

r_0, r_1 = the lengths of the upper and lower arm respectively

r_2, r_3 = the lengths of the distal and proximal links of the orthosis respectively

α = the angle between the upper arm and ground (back of wheelchair)

Θ = the angle between the upper arm and forearm

φ = the angle between the two orthosis links

ψ = the angle between the proximal orthosis link and ground (back of wheelchair)

$(0,0)$ = origin; at the point of attachment of orthosis to wheelchair

(x_1, y_1) = location of elbow (in cartesian coordinates)

(x_2, y_2) = location of terminal point (in cartesian coordinates)

as shown in Figure 3-2

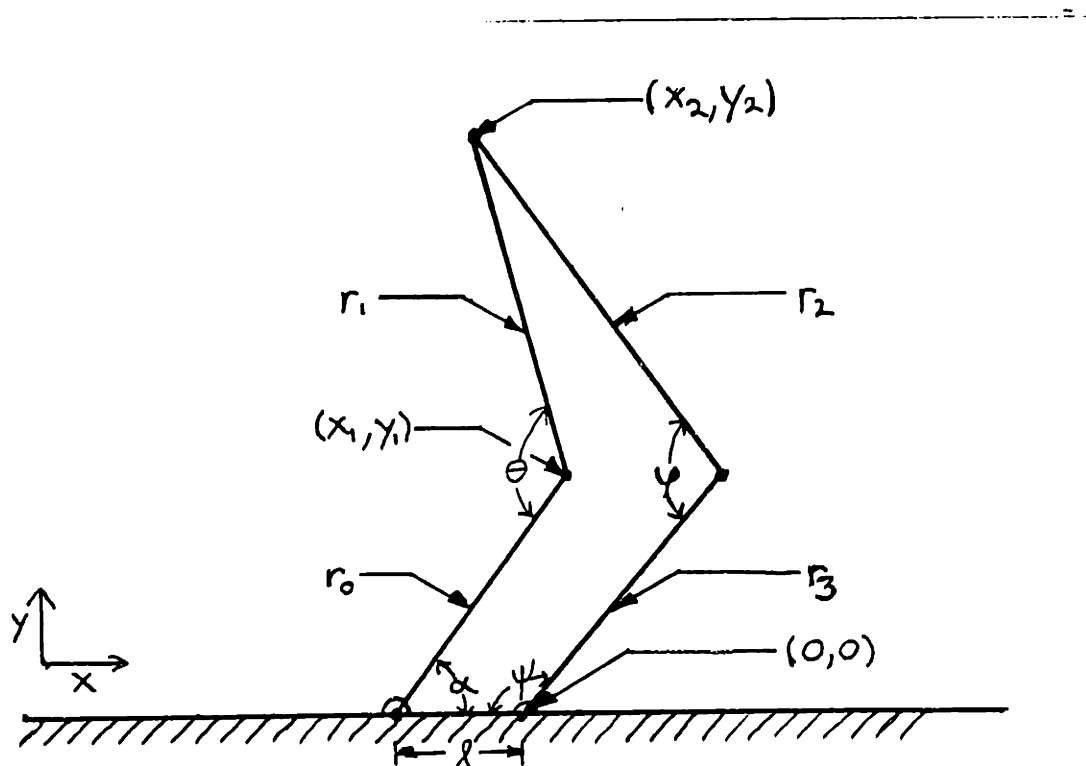


FIGURE 3-2
MODEL FOR MATHEMATICAL ANALYSIS

Although it is not actually necessary for the purposes of this thesis, the locations of the elbow and terminal point can be expressed in terms of the arm angles.

From basic trigonometric identities:

$$x_1 = r_0 \cos \alpha - l$$

$$y_1 = r_0 \sin \alpha$$

$$x_2 = r_0 \cos \alpha - l - r_1 \cos(\theta - \alpha)$$

$$y_2 = r_0 \sin \alpha + r_1 \sin(\theta - \alpha)$$

(For the purpose of this thesis, it is only necessary to know the location of the terminal point, (x_2, y_2) in cartesian coordinates.)

The angle between the two orthosis angles, ψ , is defined by the location of the terminal point, (x_2, y_2) , and the lengths of the orthosis links, r_2 and r_3 .

Using the law of cosines, and referring to Figure 3-3

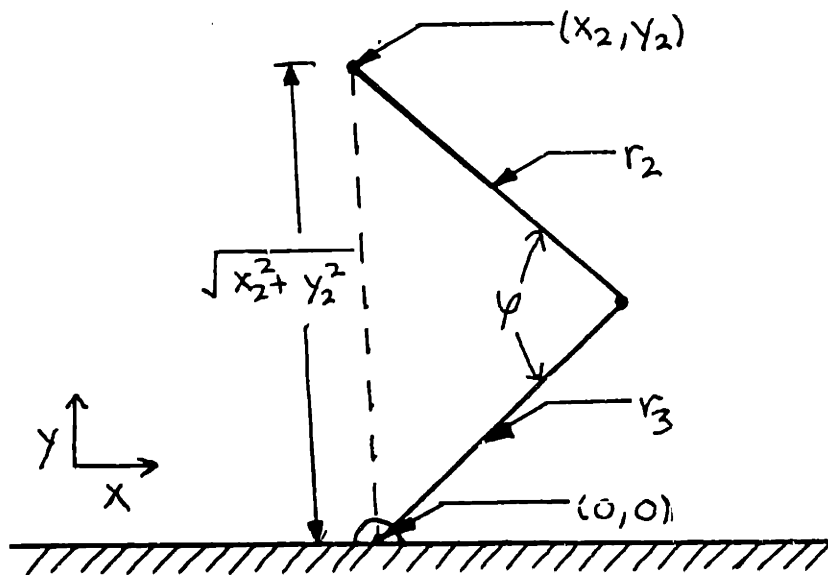


FIGURE 3-3
DERIVATION OF ψ

Since the human elbow is not a true pin joint, but rather a hinge joint, a constraint is put on ψ , to approximate the range of motion of the arm about the elbow:

$$0 \leq \psi \leq \pi$$

The angle between the proximal orthosis link and the back of the wheelchair can be defined as a sum of three angles:

$$\text{Let } \psi = \frac{\pi}{2} + G + A$$

as shown in Figure 3-4

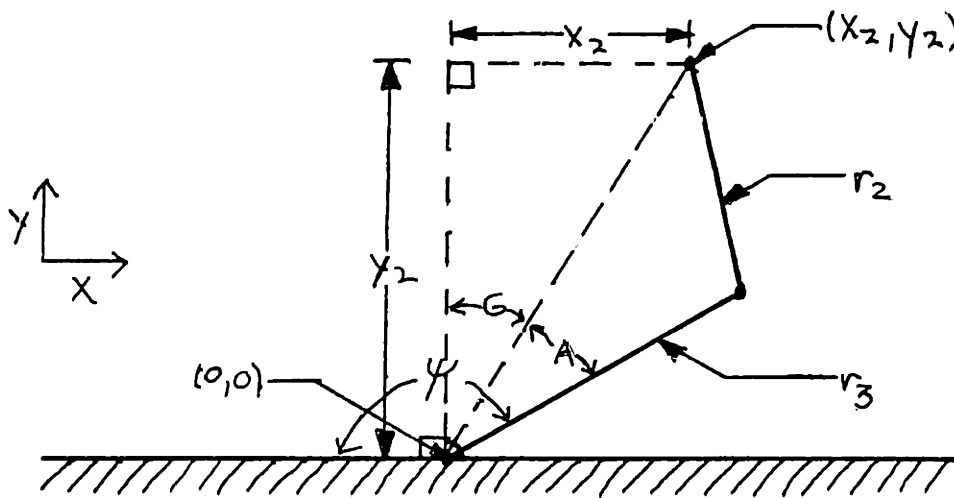


FIGURE 3-4:
DERIVATION OF ψ

By the trigonometric identity for tangent:

$$G = \tan^{-1} \left(\frac{x_2}{y_2} \right)$$

By the law of cosines

$$A = \cos^{-1} \left[\frac{(x_2^2 + y_2^2) + r_3^2 - r_2^2}{2r_3 \sqrt{x_2^2 + y_2^2}} \right]$$

Thus:

$$\psi = \frac{\pi}{2} + \tan^{-1} \left(\frac{x_2}{y_2} \right) + \cos^{-1} \left[\frac{(x_2^2 + y_2^2) + r_3^2 - r_2^2}{2r_3 \sqrt{x_2^2 + y_2^2}} \right]$$

A velocity through the terminal point, expressed as:

$$\vec{V} = \dot{x}_2 \vec{i}_2 + \dot{y}_2 \vec{j}_2$$

will produce angular velocities, $\dot{\varphi}$ and $\dot{\psi}$, at the orthosis joints, such that:

$$\dot{\varphi} = \frac{x_2 \dot{x}_2 + y_2 \dot{y}_2}{r_2 r_3 \sqrt{1 - \frac{(x_2^2 + y_2^2) - r_2^2 - r_3^2}{-2r_2 r_3}}}$$

and

$$= \frac{(y_2 \dot{x}_2 - x_2 \dot{y}_2)}{(x_2^2 + y_2^2)} - \frac{(x_2 \dot{x}_2 + y_2 \dot{y}_2)(x_2^2 + y_2^2 + r_2^2 - r_3^2)}{2r_3 (x_2^2 + y_2^2)^{3/2} \sqrt{1 - \frac{(x_2^2 + y_2^2) + r_3^2 - r_2^2}{2r_3 \sqrt{(x_2^2 + y_2^2)}}}}$$

If there are rotational viscous dampers at the orthosis joints, there will be torques produced at those joints such that:

$$T_\varphi = D_\varphi \dot{\varphi}$$

and $T_\psi = D_\psi \dot{\psi}$

where D_φ and D_ψ are the damping coefficients at the orthosis joints with angular velocities $\dot{\varphi}$ and $\dot{\psi}$ respectively.

The torques about these joints will produce a resistive force at the terminal point, which can be expressed in x and y components..

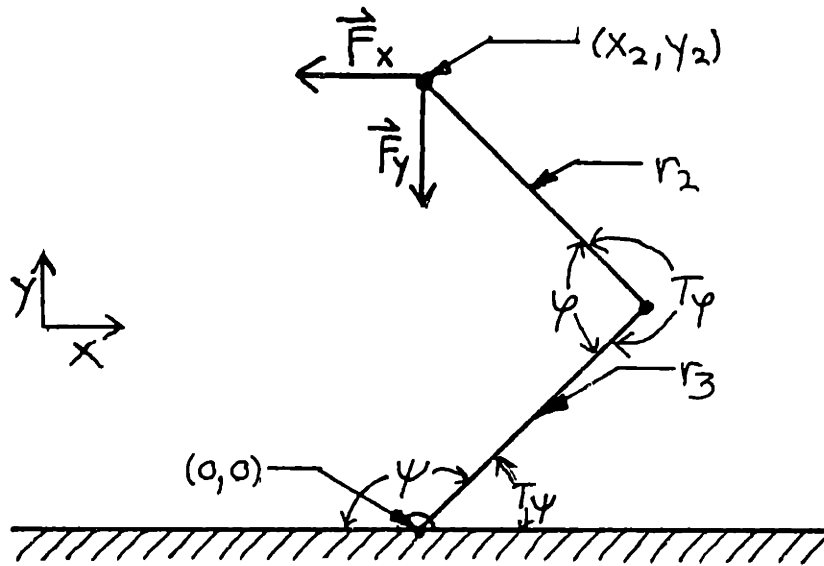


FIGURE 3-5
RESISTIVE FORCE COMPONENTS

where:

$$F_x = \frac{r_2 \cos(\varphi + \psi) T_\psi - [r_3 \cos(180 - \varphi) + r_2 \cos(\varphi + \psi)] T_\varphi}{r_2 r_3 \sin(180 - \varphi)}$$

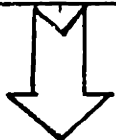
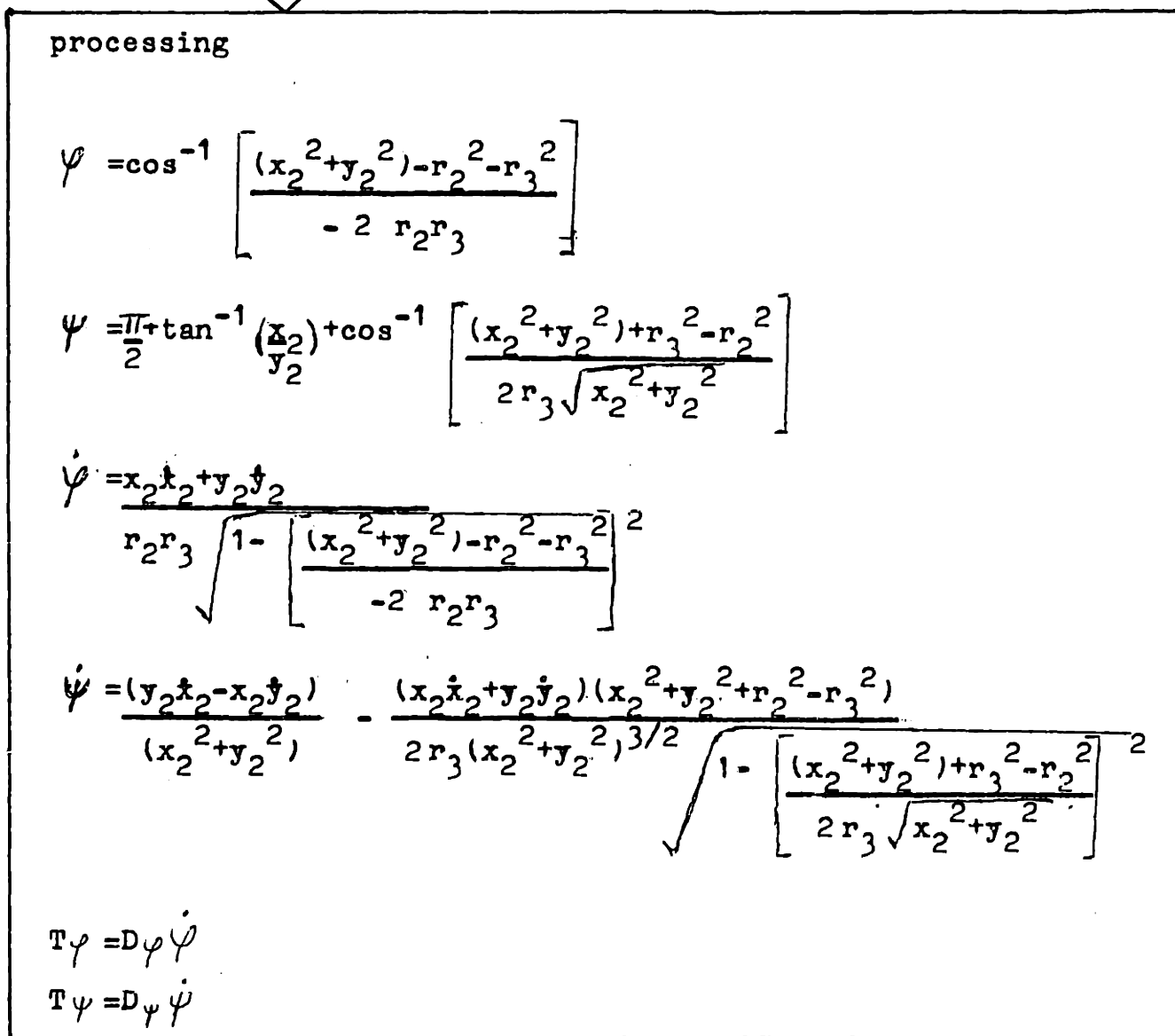
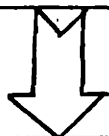
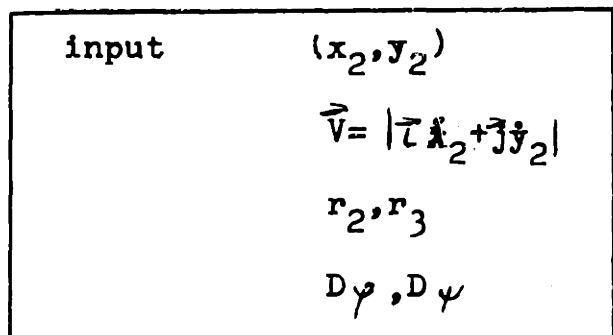
and

$$F_y = \frac{-r_2 \sin(\varphi + \psi) T_\psi - [r_3 \sin(180 - \varphi) - r_2 \sin(\varphi + \psi)] T_\varphi}{r_2 r_3 \sin(180 - \varphi)}$$

(adapted from: "Kinematics, Statics, and Dynamics of Two-D Manipulators", by Bernard K.P. Horn, June 1975, MIT AI Lab.)

Thus, given a point within the work-space of the orthosis, an instantaneous velocity through that terminal point, the length of the links of the arm restraint, and the damping coefficients at the joints, the resulting resistive force at the terminal point can be determined.

To diagram this:



output

$$F_x = \frac{r_2 \cos(\varphi + \psi) T_\varphi - [r_3 \cos(180 - \psi) + r_2 \cos(\varphi + \psi)] T_\varphi}{r_2 r_3 \sin(180 - \varphi)}$$

$$F_y = \frac{-r_2 \sin(\varphi + \psi) T_\varphi - [r_3 \sin(180 - \psi) - r_2 \sin(\varphi + \psi)] T_\varphi}{r_2 r_3 \sin(180 - \varphi)}$$

3-4 Normalization of Equations

Analysis of the force at the terminal point would be facilitated by the normalization of the determining equations. This would make a general analysis, based only on the location of the point and the direction of the velocity going through that point, as well as the link size and damping ratios, possible. Based on this analysis, a "real world" prescription, determined by the patient's tremor characteristics, limb size and strength, and task requirements, could be made on an individual basis.

What is desired are normalized equations for the force components, derived from the original equations:

$$F_x = \frac{r_2 \cos(\varphi + \psi) T_\varphi - [r_3 \cos(180 - \psi) + r_2 \cos(\varphi + \psi)] T_\varphi}{r_2 r_3 \sin(180 - \varphi)}$$

$$F_y = \frac{-r_2 \sin(\varphi + \psi) T_\varphi - [r_3 \sin(180 - \psi) - r_2 \sin(\varphi + \psi)] T_\varphi}{r_2 r_3 \sin(180 - \varphi)}$$

First, the size of the links can be normalized so that it can be expressed in terms of a size ratio and factor.

Let $r_{30} \equiv 1$

and $r_{20} \equiv R$ where R is the dimensionless ratio of link lengths

so $r_3 = R$

$r_2 = KR$ where K is the link size factor in units of length (L)

The velocity at the terminal point can also be normalized:

$$|\vec{V}| = |\vec{i} \dot{x}_2 + \vec{j} \dot{y}_2|$$

where \vec{V} is the velocity vector, and \dot{x}_2 and \dot{y}_2 are the components

\vec{V} can be expressed in terms of magnitude and direction:

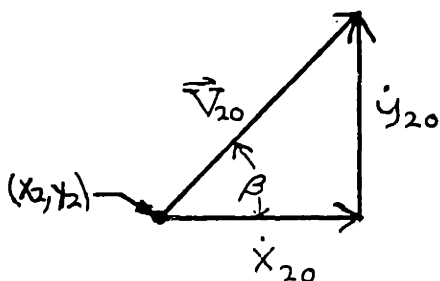


FIGURE 3-6
NORMALIZATION OF
TERMINAL VELOCITY

Let: $\dot{x}_{20} \equiv 1$

and $\dot{y}_{20} \equiv \tan \beta$

where β is the angle of the velocity vector

Thus: $\dot{x}_2 = \vec{V}$

and $\dot{y}_2 = \vec{V} \tan \beta$

where V is the velocity magnitude in units of length and inverse time (L/T)

The distance to the terminal point can be expressed in terms of the fraction of the total reach of the orthosis:

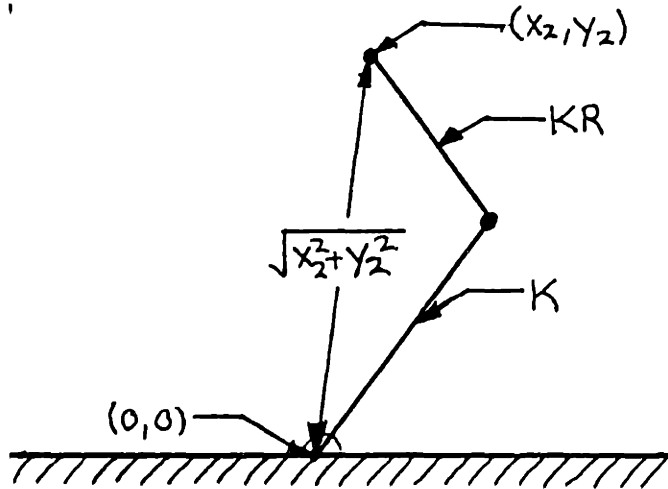


FIGURE 3-7
NORMALIZED DISTANCE
TO TERMINAL POINT

$r = \frac{\text{distance to terminal point}}{\text{total reach of orthosis}}$

$$P = \frac{\sqrt{x_2^2 + y_2^2}}{K(1+R)}$$

where P is a dimensionless ratio

The terminal point can be defined in terms of the direction from the origin, and the distance to that point.

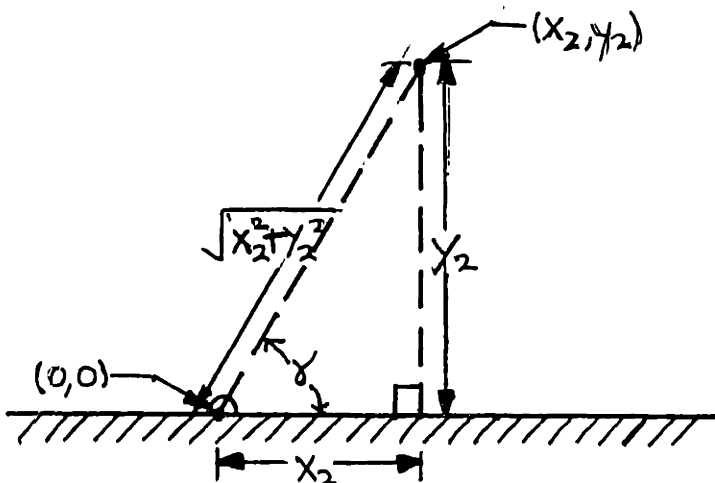


FIGURE 3-8
ANGLE TO TERMINAL POINT

where γ is the angular direction from the origin to the terminal point

$$0 \leq \gamma \leq \pi$$

$$\text{So: } x_2 = \cos \gamma (\sqrt{x_2^2 + y_2^2})$$

$$y_2 = \sin \gamma (\sqrt{x_2^2 + y_2^2})$$

$$\frac{y_2}{x_2} = \tan \gamma; \quad \frac{x_2}{y_2} = \tan\left(\frac{\pi}{2} - \gamma\right)$$

Combining expressions:

$$x_2 = \cos \gamma (KP)(1+R)$$

$$y_2 = \sin \gamma (KP)(1+R)$$

These normalized values can be substituted into the expressions for the angles at the orthosis joints.

From before:

$$\psi = \cos^{-1} \left[\frac{(x_2^2 + y_2^2) - r_2^2 - r_3^2}{-2r_2r_3} \right]$$

$$\psi = \frac{\pi}{2} + \tan^{-1} \left(\frac{x_2}{y_2} \right) + \cos^{-1} \left[\frac{(x_2^2 + y_2^2) + r_3^2 - r_2^2}{2r_3\sqrt{x_2^2 + y_2^2}} \right]$$

Making the substitutions and simplifying:

$$\psi = \cos^{-1} \left[\frac{P^2(1+R)^2 - (R^2+1)}{-2R} \right]$$

and

$$\psi = \pi - \gamma + \cos^{-1} \left[\frac{P^2(1+R)^2 + (1-R^2)}{2P(1+R)} \right]$$

Since, by the law of cosines,:

$$(x_2^2 + y_2^2) = k^2(R^2 + 1 - 2R \cos \psi)$$

ψ can also be expressed as:

$$\psi = \pi - \gamma + \cos^{-1} \left[\frac{(1 - R \cos \psi)}{\sqrt{R^2 + 1 - 2R \cos \psi}} \right]$$

Similar substitutions can be made for the expressions for the angular velocities.

Thus:

$$\dot{\psi} = \frac{V}{K} \left[\frac{R(1+R)(\cos \delta + \sin \delta \tan \beta)}{R \sin \psi} \right]$$

and

$$\dot{\psi} = \frac{V}{K} \left(\frac{R(1+R)}{R^2 + 1 - 2R \cos \psi} \right) \left[(\sin \delta - \cos \delta \tan \beta) - \frac{(\cos \delta + \sin \delta \tan \beta)(R - \cos \psi)}{\sin \psi} \right]$$

($\dot{\psi}$ and $\dot{\psi}$ are in units of $\frac{LT^{-1}}{L} = T^{-1}$)

The damping coefficients may also be normalized:

Let: $D_{\varphi 0} \equiv 1$

where B is the dimensionless ratio of damping coefficient

and $D_{\psi 0} \equiv B$

where D is the damping factor (in units of $F \cdot LT$)

Using the expressions for torque

$$T_{\varphi} = D_{\varphi} \dot{\psi}$$

$$T_{\psi} = D_{\psi} \dot{\psi}$$

and substituting normalized expressions for D_{φ} and D_{ψ} , and defining,

$$\dot{\psi} = \frac{V}{K} [\dot{\psi}^*]$$

($[\dot{\psi}^*]$ and $[\dot{\psi}^*]$ are dimensionless)

$$\dot{\psi} = \frac{V}{K} [\dot{\psi}^*]$$

The torques can be expressed in normalized expressions:

$$T_{\psi} = \frac{DV}{K} [\dot{\psi}^*]$$

and $T_{\psi} = \frac{DV}{K} B [\dot{\psi}^*]$

The normalized expressions may now be substituted into the equations for the x and y force components:

$$F_x = \frac{DV}{K^2} \left(\frac{R \cos(\psi + \Psi) B [\dot{\psi}^*] - [\cos(180 - \Psi) + K \cos(\psi + \Psi)] [\dot{\psi}^*]}{R \sin(180 - \Psi)} \right)$$

and

$$F_y = \frac{DV}{K^2} \left(\frac{-R \sin(\psi + \Psi) B [\dot{\psi}^*] - [\sin(180 - \Psi) - R \sin(\psi + \Psi)] [\dot{\psi}^*]}{R \sin(180 - \Psi)} \right)$$

and, by defining:

$$\left[F_x^* \right] = \left(\frac{K^2}{DV} \right) F_x$$

and

$$\left[F_y^* \right] = \left(\frac{K^2}{DV} \right) F_y$$

Completely dimensionless expressions for the force components are obtained.

3-5 Summary of Normalized Equations

Independent variables

$$P, \gamma, \beta$$

Controlling parameters

$$B, R$$

$$\varphi = \cos^{-1} \left[\frac{P^2(1+K)^2 - (K^2+1)}{-2K} \right]$$

$$\psi = \pi - \gamma + \cos^{-1} \left[\frac{P^2(1+K)^2 + (1-R^2)}{2P(1+K)} \right]$$

$$[\dot{\varphi}^*] = \frac{K(1+K)(\cos \gamma + \sin \gamma \tan \beta)}{R \sin \varphi}$$

$$[\dot{\psi}^*] = \left(\frac{P(1+K)}{K^2+1-2R\cos\varphi} \right) \left[(\sin \gamma - \cos \gamma \tan \beta) - \frac{(\cos \gamma + \sin \gamma \tan \beta)(R - \cos \varphi)}{\sin \varphi} \right]$$

$$[F_x^*] = \frac{K \cos(\varphi + \psi) B [\dot{\psi}^*] - [\cos(\pi - \psi) + K \cos(\varphi + \psi)] [\dot{\varphi}^*]}{R \sin(\pi - \varphi)}$$

$$[F_y^*] = \frac{-K \sin(\varphi + \psi) B [\dot{\psi}^*] - [\sin(\pi - \psi) - R \sin(\varphi + \psi)] [\dot{\varphi}^*]}{R \sin(\pi - \varphi)}$$

Chapter 4- Results

4-1 Introduction

Results of the system analysis were obtained using software written for the VAX computer at the MIT Joint Computer Facility. Plots were obtained showing the relative magnitudes and directions of the resistive force components for various specified independent variables and system parameters. The force components are shown within a defined work-space, with a radius of one dimensionless unit.

Several examples are included and discussed in this section. All other plots, and the software which generated them, are located in the Appendices A and B.

4-2 Verification of Results

In order to verify that the force components shown in the plots represent the actual components, two cases are presented, one special, and one general.

4-2-1 Special Case

In the case where the applied velocity vector is axial to the proximal link of the restraint and perpendicular to the distal link, the resistive force should be entirely a result of the action of the distal damper, and should have no horizontal component. This can be ascertained by choosing variable and parameter values which will yield such a configuration.

Letting $R=1$, $B=1$, $\beta = \pi/4$, $\gamma = \pi/2$, and $P= 0.5$, and using the equations derived in Chapter 2:

$$\varphi = \cos^{-1} \left[\frac{(0.5)^2(1+1)^2 - (1^2+1)}{-2(1)} \right]$$

$$\varphi = \pi/2$$

$$\psi = \pi - \gamma - \cos^{-1} \left[\frac{(0.5)^2(1+1)^2 + (1-1^2)}{2(0.5)(1+1)} \right]$$

$$\psi = 3\pi/4$$

$$[\dot{\varphi}^*] = \frac{(0.5)(1+1)(\cos \pi/2 - \sin \pi/2 \tan \pi/4)}{(1)\sin \pi/2}$$

$$[\dot{\varphi}^*] = 1.414$$

$$[\dot{\psi}^*] = \frac{(0.5)(1+1)(\sin \pi/2 + \cos \pi/2 \tan \pi/4) - (\cos \pi/2 + \sin \pi/2 \tan \pi/4)(1 - \cos \pi/2)}{1^2 + 1 - 2(1)\cos \pi/2} \cdot \frac{1}{\sin \pi/2}$$

$$[\dot{\psi}^*] = 0$$

Since the joint-torque is proportional to the angular velocity, there is no torque at the proximal joint.

So, to compute the force components:

$$[F_x^*] = \frac{(1)\cos 5\pi/4(1)(0) - (\cos \pi/4 + \cos 5\pi/4)(1.414)}{(1)\sin \pi/2}$$

since $\cos \pi/4 = -\cos 5\pi/4$

$$[F_x^*] = 0 \text{ There is no horizontal force component}$$

However, there is a vertical force component:

$$[F_y^*] = \frac{(-1)\sin 5\pi/4(1)(0) - (\sin \pi/4 - \sin 5\pi/4)(1.414)}{(1)\sin \pi/2}$$

$$[F_y^*] = -2$$

The configuration of this special case is shown in Figure 4-1, and the resistive force components calculated with the computer program are shown in Figure 4-2.

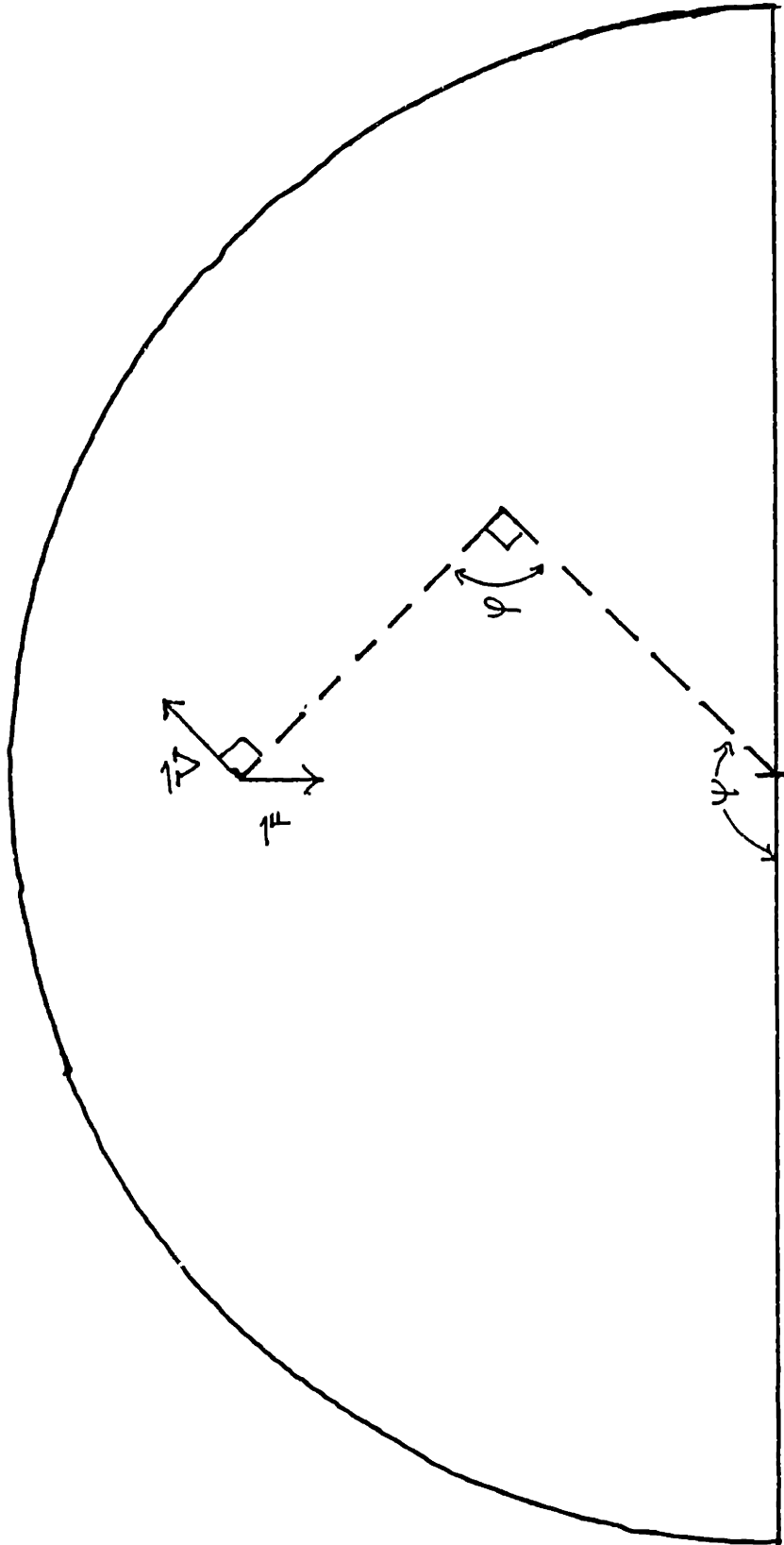
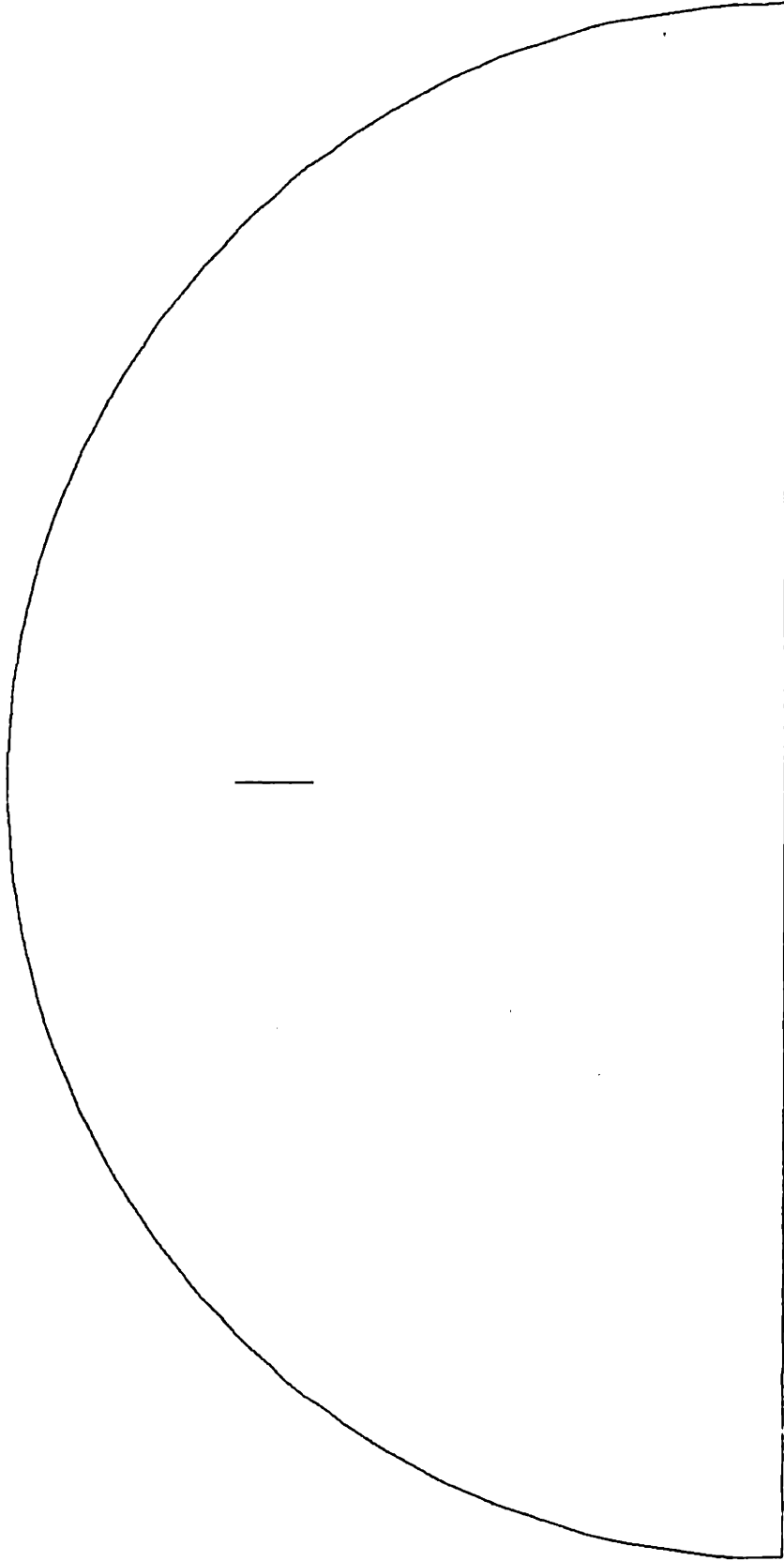


FIGURE 4-1

CONFIGURATION OF
A SPECIAL CASE

$\beta = 45^\circ$
 $R = 1$
 $B = 1$
 $\psi = 135^\circ$
 $\varphi = 90^\circ$



$P = 0.7071$
 $R = 1.0$
 $B = 1.0$
 $\beta = 45^\circ$
 $\psi = 135^\circ$
 $\varphi = 90^\circ$
 $\gamma = 90^\circ$

FIGURE 4-2
PLOT OF NORMALIZED
FORCE COMPONENTS
FOR A SPECIAL CASE

4-2-2 General Case

The configurations of two plots are considered. In each plot, the links have a length ratio of one, and a damping ratio of one. The damped velocity is applied at an angle of $\pi/4$ radians.

In plot 1, the terminal point is at an angle of $5\pi/12$ radians at a distance of 0.66 units. As shown in Figure 4-3, the velocity vector is closer to being perpendicular to the distal link than to the proximal link. Based on intuition, and what was shown previously in the special case, it would be expected that the vertical component of the resistive force would be larger than the horizontal component. This is verified by the components plotted by the computer.

The opposite is true in plot2, with the terminal point at angle of $5\pi/6$ radians and a distance of 0.8 units. The velocity vector is more perpendicular to the distal link, and, hence, the horizontal force component is larger.

Thus, it can be seen that the plots do correspond to the actual behavior of the force components.

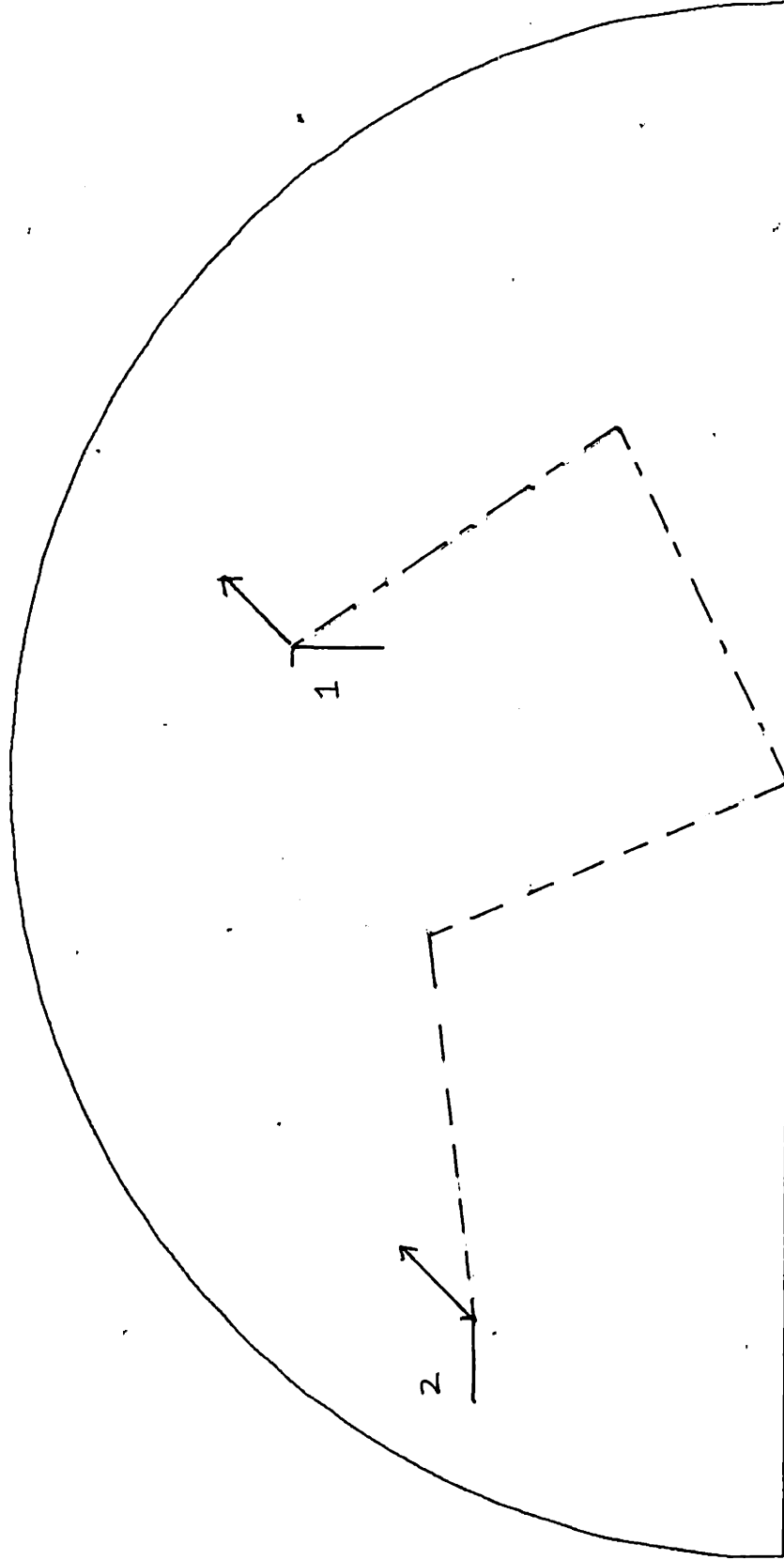


FIGURE 4-3
GENERAL CASE

$$R=1.0; B=1.0; \beta = \pi/4$$

4-3 Interpretation of Results

4-3-1 Reading of Plots

The results are plotted in an area representing the work-space of the orthosis, where the radius of the semi-circle is the total reach of the orthosis. Normalized force components are shown for velocities at different points within the area. Unless noted otherwise, the points are at angle increments of 15 degrees along radii representing 33%, 50%, 66%, and 80% of the total reach. The link length and damping ratios, and the angle of the velocity vector are noted.

4-3-2 Ideal Damping

Ideal damping has been defined as being omni-directional, such that the resistive force vector is axial to the applied velocity vector. If the angular difference between the velocity and force vectors is defined as δ , ideal damping is achieved at $\delta = 0$.

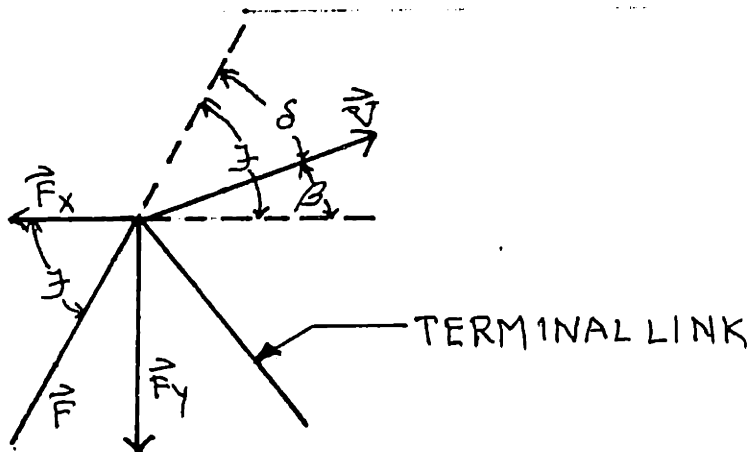


FIGURE 4-4
DERIVATION OF δ

where $\zeta = \tan^{-1} \frac{[F_y^*]}{[F_x^*]}$

and $\delta = \zeta - \beta$

So, in the case where $\beta = \pi/4$, ideal damping is achieved where

$[F_y^*] = [F_x^*]$

Figure 4-5 shows points where ideal damping is achieved for a velocity vector at 45 degrees, and Figure 4-6 shows ideal damping at various vector angles. In both cases, $R=1$ and $B=1$.

Consequently, for any given set of parameters and independent variables, the angle of the velocity vector at which there is ideal damping can be predicted using:

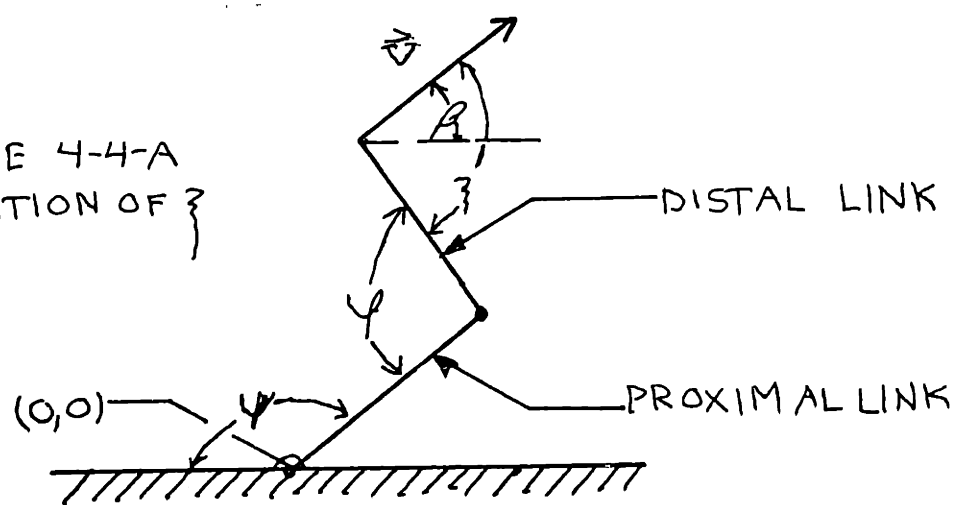
$$\frac{R \cos(\psi + \varphi) B [\dot{\psi}^*] - [\cos(\pi - \varphi) + R \cos(\psi + \varphi)] [\dot{\psi}^*]}{R \sin(\pi - \varphi)}$$

$$= \frac{-R \sin(\psi + \varphi) B [\dot{\psi}^*] - [\sin(\pi - \varphi) - \sin(\psi + \varphi)] [\dot{\psi}^*]}{R \sin(\pi - \varphi)}$$

For the case when $R=1$ and $B=1$, a relationship can be noted between the angle between the velocity vector and the terminal link. (ζ)

where $\zeta = \psi + \varphi - \pi + \beta$

FIGURE 4-4-A
DERIVATION OF ζ



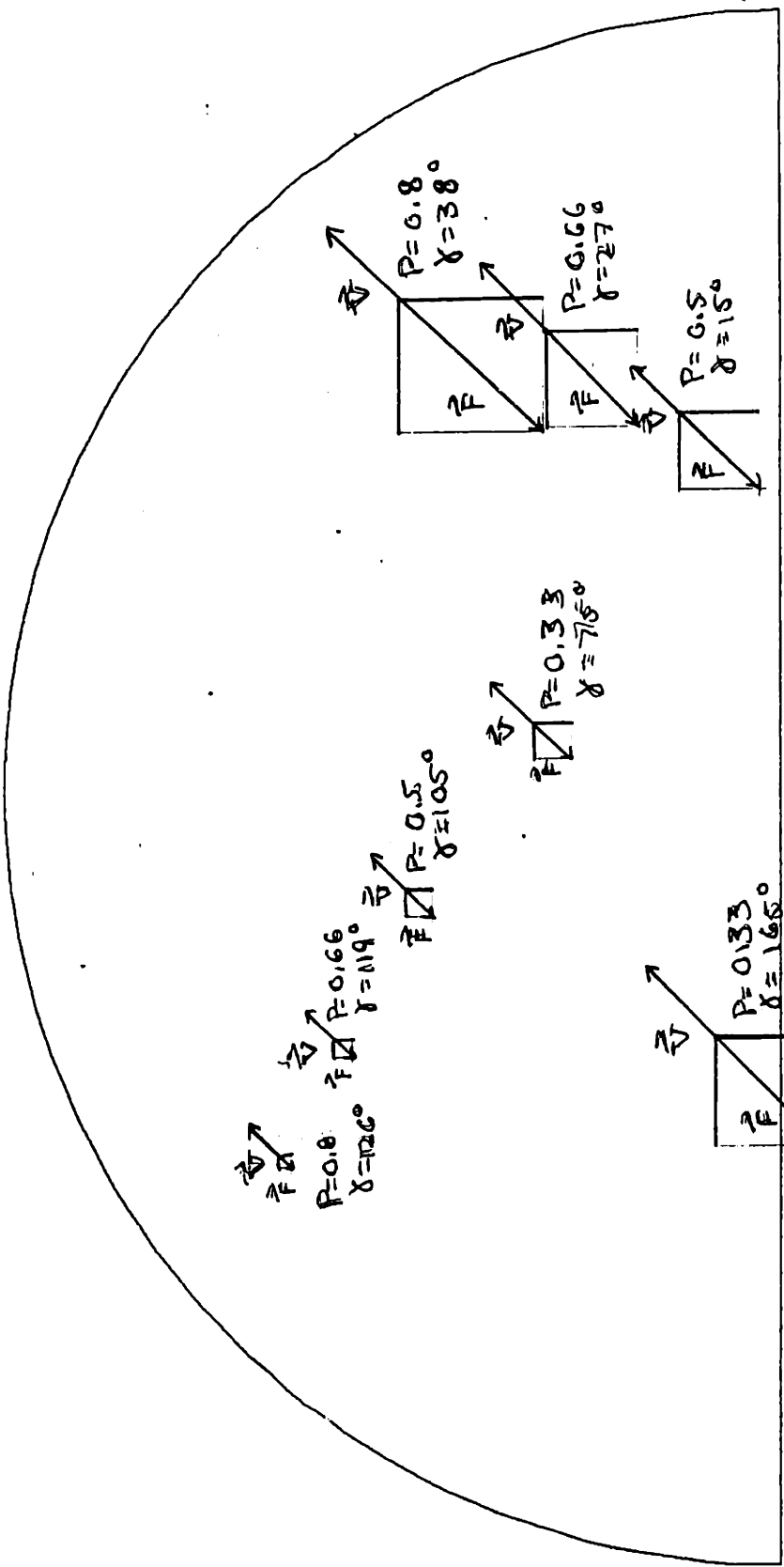


FIGURE 4.5
IDEAL DAMPING AT $\beta = \pi/4$

$R=1.0; \beta=1.0; \beta = \pi/4$

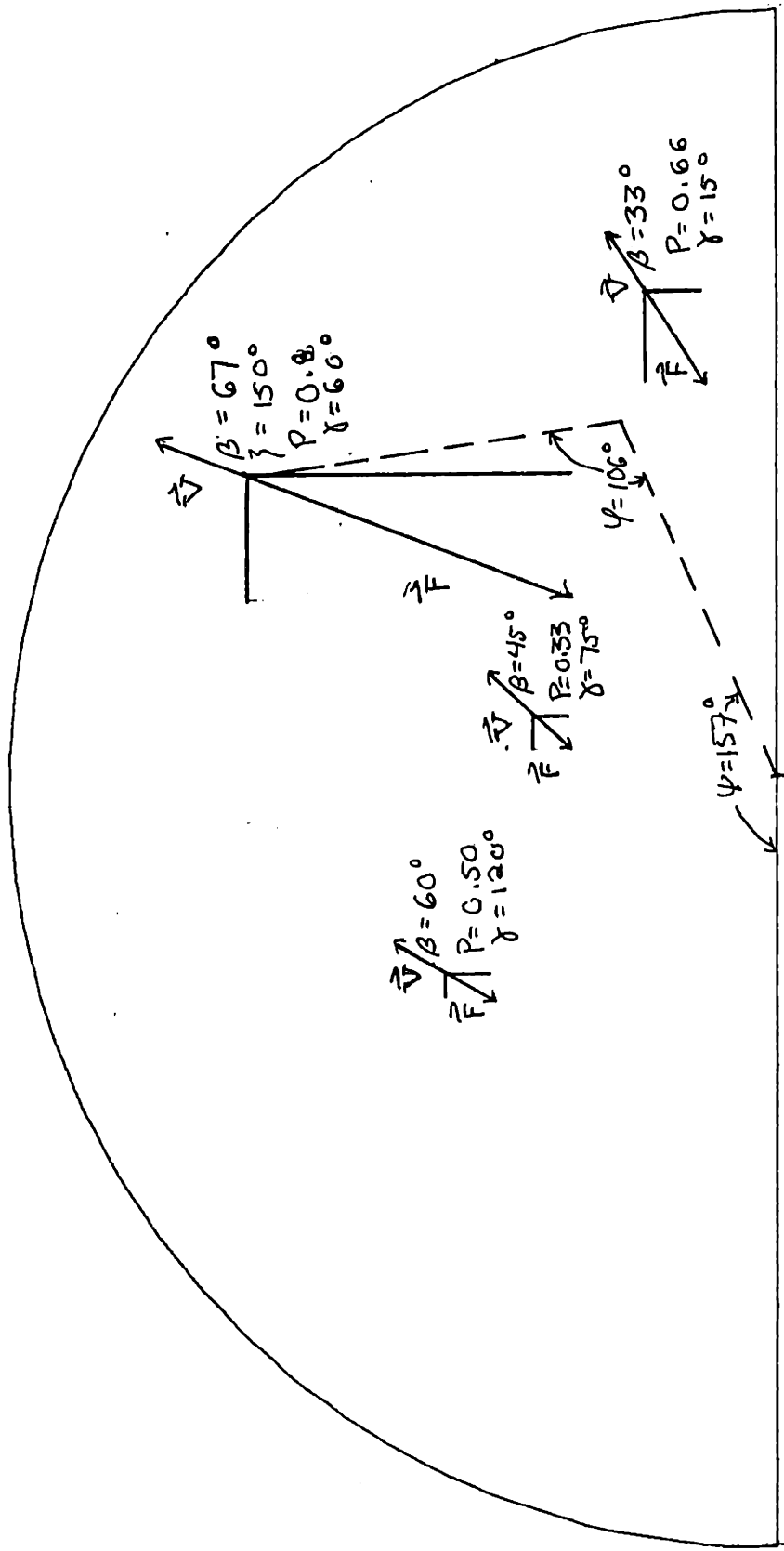


FIGURE 4.6
 IDEAL DAMPING AT VARIOUS VALUES OF β
 SHOWING THE RESTRAINT CONFIGURATION FOR ONE POINT

$R=1, B=1$

Data For Figure 4-5

Table 4-1

$R=1, B=1, \beta = 45^\circ$

P in dimensionless units

$\varphi, \psi, \gamma, \zeta$, in degrees

P	φ	ψ	γ	ζ
0.33	39	176	75	80
0.33	39	86	165	-10
0.50	60	225	15	150
0.50	60	135	105	60
0.66	83	202	27	150
0.66	83	110	119	58
0.80	106	179	38	150
0.80	106	91	126	62

Data For Figure 4-6

Table 4-2

$R=1, B=1$

P in dimensionless units

$\varphi, \psi, \gamma, \beta, \zeta$, in degrees

P	φ	ψ	γ	β	ζ
0.33	39	176	75	45	80
0.50	60	120	120	60	60
0.66	83	214	15	33	150
0.80	106	157	60	67	150

This relationship is plotted in Figure 4-7 for three values of P. Figure 4-7 shows that the deviation from ideal damping increases for larger values of P, especially above $P=0.5$.

This can also be seen in Figure 4-8, which shows the normalized force components at distances representing 33%, 50%, 66%, and 80% of the total restraint reach, where $R=1$, $B=1$, and $\beta = \pi/4$. Thus, the best damping characteristics would be obtained with a restraint that is substantially larger than the arm. Consequently, independent restraint of each arm joint is not feasible, since it would require that the arm length and orthosis length be coincident.

4-3-3 Effects of Varying Parameters

When the two restraint links are not the same length, the results become inconsistent, and the area in which there is ideal damping decreases dramatically. Cases in which the distal link is shorter and in which the proximal link is shorter are shown in Figures 4-9 and 4-10 respectively. Consequently, it can be concluded that a one-to-one ratio of link lengths is optimal for this application.

The effect of varying the damping ratio is less dramatic, but more informative. By changing the damper ratio, ideal damping can be obtained at points in the work-space where otherwise it could not be achieved. Cases in which the distal joint has a larger damping coefficient and in which the proximal joint has a larger damping coefficient are shown in Figures 4-11 and 4-12 respectively. Thus, it can be concluded that the best damping characteristics would be obtained with adjustable dashpot with feedback control,

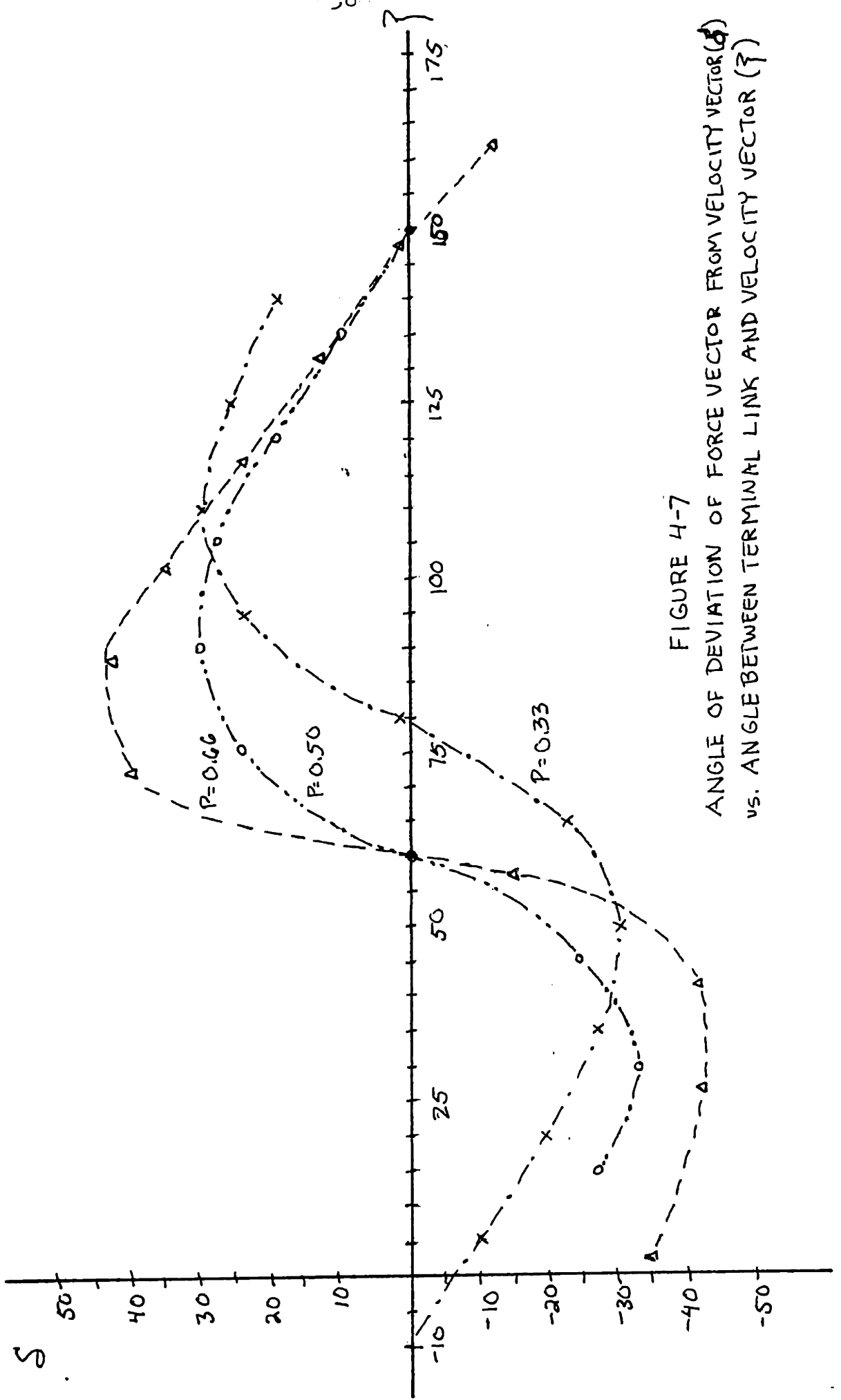


FIGURE 4-7

ANGLE OF DEVIATION OF FORCE VECTOR FROM VELOCITY VECTOR (δ)
 vs. ANGLE BETWEEN TERMINAL LINK AND VELOCITY VECTOR (γ)

Data For Figure 4-7

Table 4-3

$B=1, R=1, \beta=45^\circ$

(all angles in degrees)

P	ψ	Ψ	γ	\bar{r}	F_y/F_x	\bar{r}	δ
0.33	39	236	15	140	2.03	64	19
0.33	39	221	30	125	2.96	71	26
0.33	39	206	45	110	3.66	75	30
0.33	39	191	60	95	2.59	69	24
0.33	39	176	75	80	1.02	46	1
0.33	39	161	90	65	0.40	22	-23
0.33	39	146	105	50	0.27	15	-30
0.33	39	131	120	35	0.33	18	-27
0.33	39	116	135	20	0.48	26	-19
0.33	39	101	150	5	0.69	35	-10
0.33	39	86	165	-10	0.99	45	0
0.5	60	225	15	150	1.01	45	0
0.5	60	210	30	135	1.41	55	10
0.5	60	295	45	120	2.07	64	19
0.5	60	180	60	105	3.03	72	27
0.5	60	165	75	90	3.73	75	30
0.5	60	150	90	75	2.57	72	24
0.5	60	135	105	60	1.00	45	0
0.5	60	120	120	45	0.39	23	-24
0.5	60	105	135	30	0.21	14	-33
0.5	60	90	150	15	0.33	17	-27
0.5	60	75	165	0	0.49	27	-19
0.66	83	214	15	162	0.66	33	-12
0.66	83	199	30	147	1.02	46	1
0.66	83	184	45	132	1.58	58	13
0.66	83	169	60	117	2.68	69	24
0.66	83	154	75	102	5.68	80	35
0.66	83	139	90	87	28.50	88	43
0.66	83	124	105	72	11.20	85	40
0.66	83	109	120	57	0.58	30	-15
0.66	83	94	135	42	0.06	4	-41
0.66	83	79	150	27	0.05	3	-42
0.66	83	64	165	12	0.19	11	-34

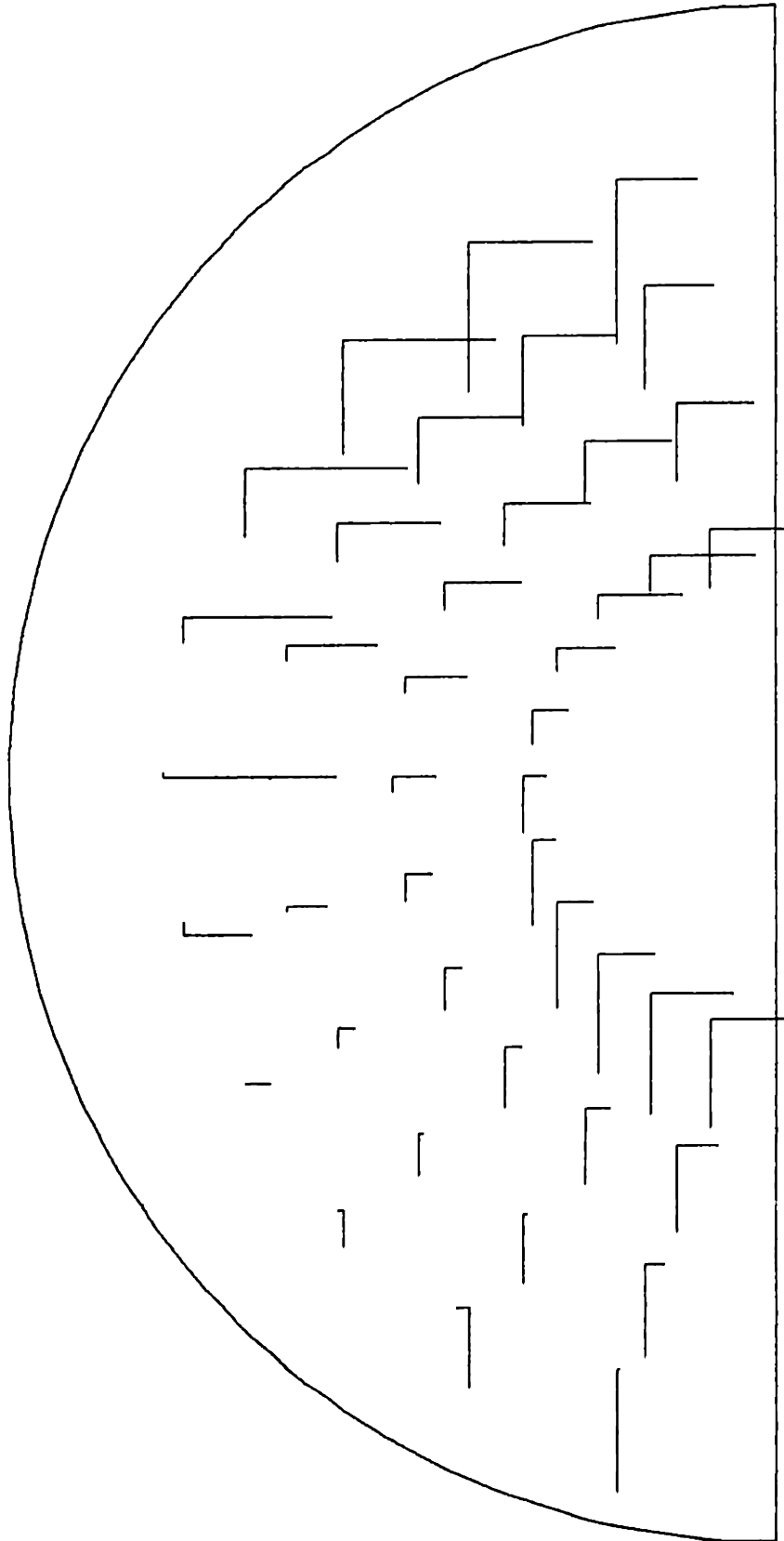
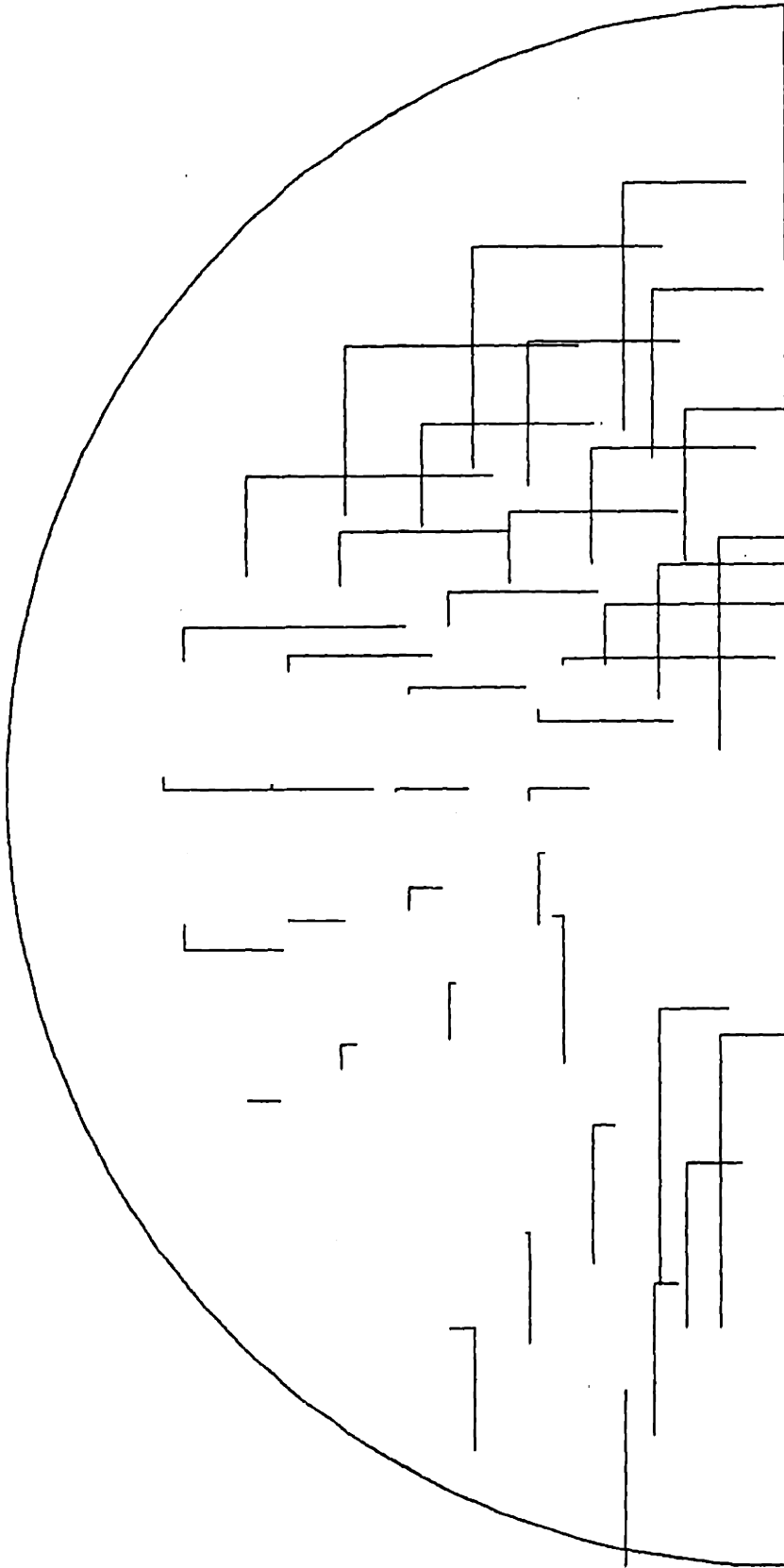


FIGURE 4-8

PLOTS OF NORMALIZED
FORCE COMPONENTS FOR
EQUAL LINKS AND DAMPERS

$R=1, \beta=1, \beta=\pi/4$



$KR=1.2$; $R=0.75$; $B=1.0$; $\beta=\pi/4$

FIGURE 4-9

PLOTS OF NORMALIZED
FORCE COMPONENTS WITH
DISTAL LINK SHORTER

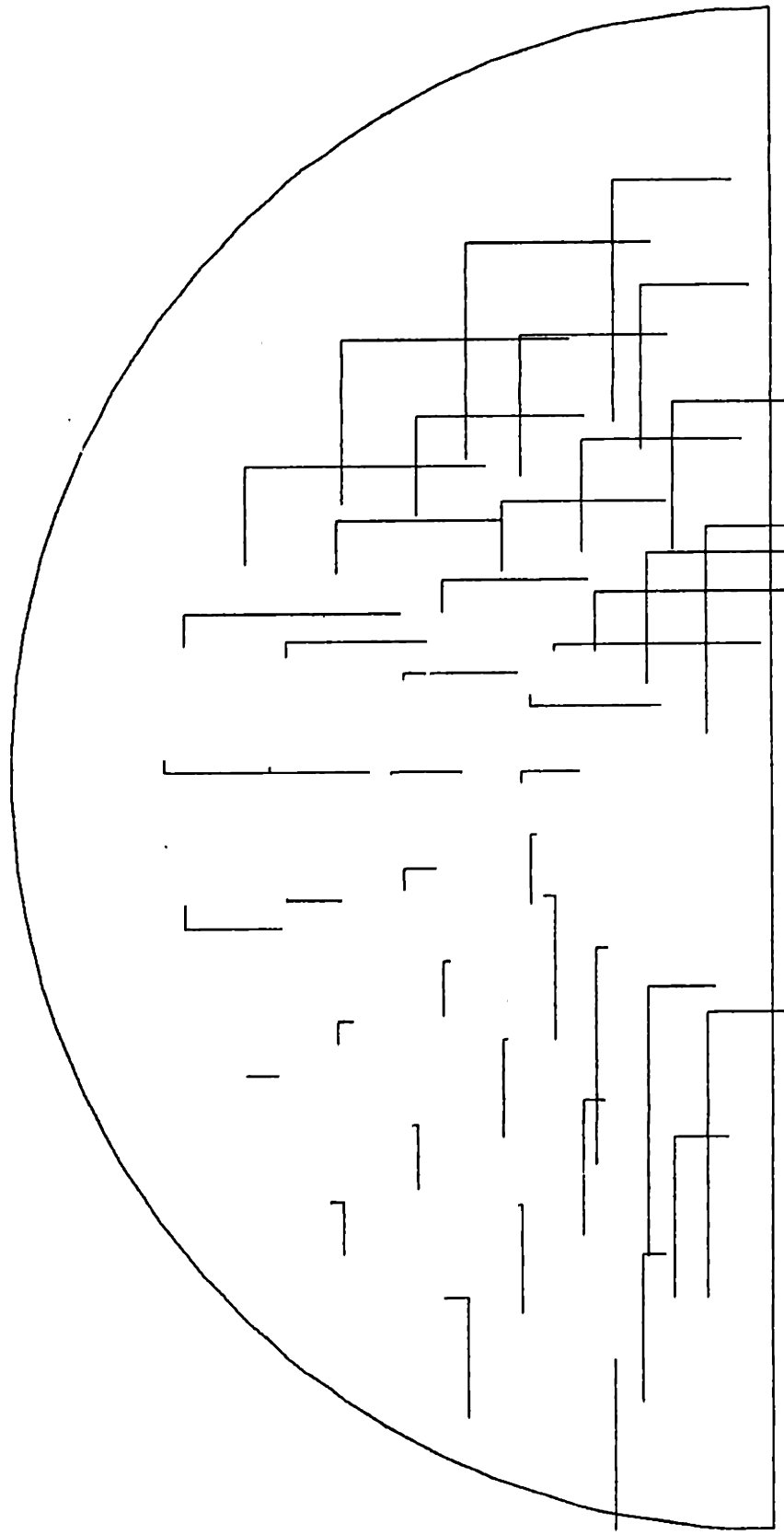


FIGURE 4-10
PLOTS OF NORMALIZED
FORCE COMPONENTS WITH
PROXIMAL LINK SHORTER

$KR = r_3; R = 0.75; B = 1.0; \beta = \pi/4$

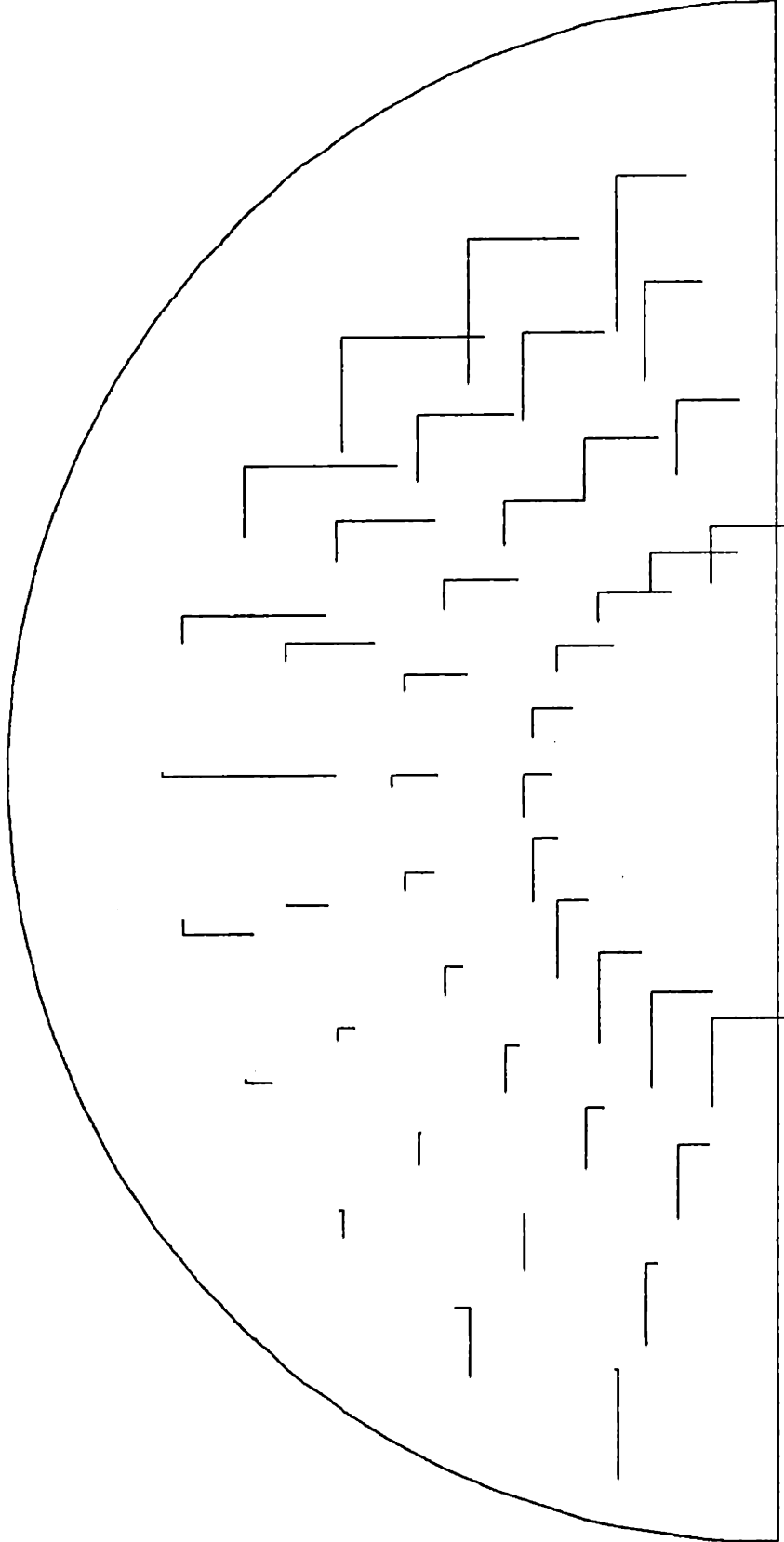
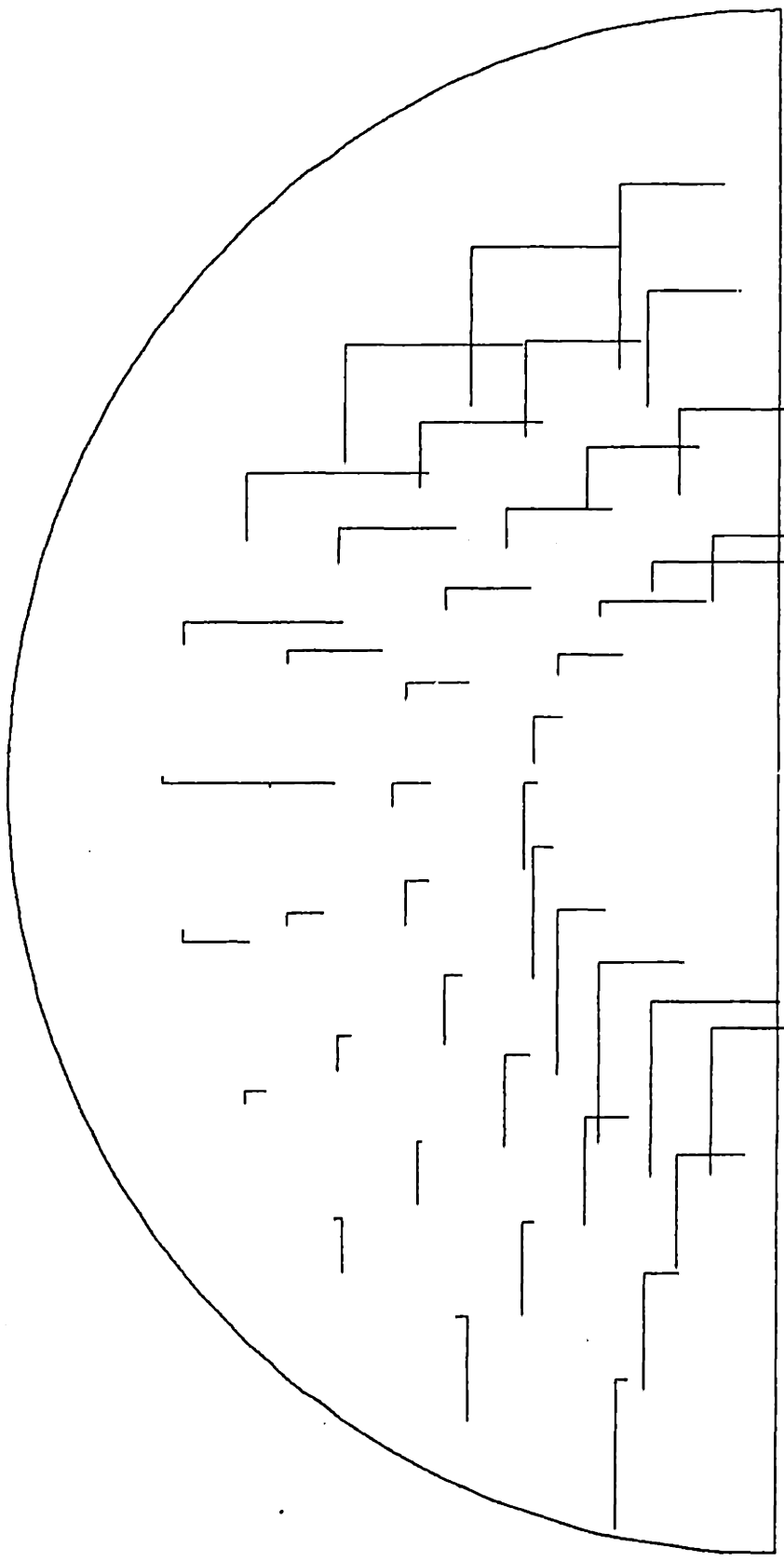


FIGURE 4-11
PLOTS OF NORMALIZED
FORCE COMPONENTS WITH
MORE DAMPING AT DISTAL JOINT

$KR = r_2; R = 1.0, \beta = 0.75, \beta = \pi/4$



$KR = r_2; R = 1.0; B = 1.5; \beta = \pi/4$

FIGURE 4-12
PLOTS OF NORMALIZED
FORCE COMPONENTS WITH
MORE DAMPING AT PROXIMAL JOINT

which would adjust the damping ratio to provide ideal damping at every configuration.

Chapter 5- Summary and Conclusions

The analysis determined that the most consistent damping behavior is obtained with a restraint with links of equal length. It was also shown that the extent of ideal, omni-directional damping can be varied by adjusting the damping coefficients at two restraint joints. A restraint reach greater than that of the arm was found to be preferable, so independent restraint of each arm joint was determined to not be feasible, since it would require that the restraint and the arm be completely coincident. Consequently, the ball-bearing feeder is not an acceptable basis for the restraint design.

Thus, it can be concluded that with a fixed-base compliant restraint for the suppression of arm tremor during precision movements within a work-space, the best damping characteristics would be obtained with a restraint of equal length links, a reach of approximately twice that of the arm, and variable continuous rotational viscous dampers with feedback control providing positional and directional information.

Appendix A

Computer Program Listings

```

C THIS PROGRAM IS DESIGNED TO PLOT THE NORMALIZED FORCE COMPONENTS
C COMPUTED IN THE SUBROUTINE FORCES.
C
C INITIALIZE THE PLOTTING DEVICE.
C
C     CALL T4625
C
C DETERMINE THE LOCATION OF THE PLOT ON THE PAGE AND THE AREA IT
C WILL OCCUPY. "SHOW" WILL GIVE SQUARE COORDINATES.
C
C     CALL LOCATE(10.,90.,10.,90.)
C     CALL SHOW(-1.,1.,0.,1.)
C
C DRAW THE WORK-SPACE
C
C     CALL MOVE(-1.,0.)
C     CALL DRAW(1.,0.)
C     PI=3.14159
C     DO 10 X=0.,PI,PI/100.
C     CALL DRAW(COS(X),SIN(X))
10  CONTINUE
C
C CALL THE SUBROUTINE WHICH WILL CALCULATE THE COMPONENTS OF
C THE NORMALIZED FORCE VECTORS AND PLOT THEM.
C
C     CALL FORCES
C
C END THE PLOTTING ROUTINE
C
C     CALL ENDPLT
C     END

```

3 THIS PROGRAM IS DESIGNED TO COMPUTE THE RELATIVE MAGNITUDES OF THE
 C X AND Y COMPONENTS OF A NORMALIZED FORCE AT THE TERMINAL POINT ON
 C A VISCOUSLY DAMPED AND RESTRAINT, GIVEN THE LOCATION OF THE TERMINAL
 C POINT, THE DIRECTION OF THE DAMPED VELOCITY VECTOR, AND THE RATIOS FOR
 C THE RESTRAINT LINK LENGTHS AND DAMPERS.

SUBROUTINE FORCES
 INTEGER REPLY, I, J, K
 PI=3.14159

5 SPECIFY THE RATIOS OF THE CONTROLLING PARAMETERS, R AND B

10 WRITE(6,10)
 15 FORMAT(' WHAT IS THE SIZE RATIO OF THE LINKS?')
 20 READ(5,15)R
 25 FORMAT(F8.4)
 30 WRITE(6,20)
 35 FORMAT(' WHAT IS THE DAMPER RATIO?')
 40 READ(5,25)B
 45 FORMAT(F8.4)

50 SPECIFY THE INDEPENDENT VARIABLES, GAMMA, H, AND BETA

55 WRITE(6,35)
 60 FORMAT(' WHAT IS THE DIRECTION OF THE TERMINAL POINT?')
 65 READ(5,40)GAMMA
 70 FORMAT(F6.5)
 75 WRITE(6,45)
 80 FORMAT(' WHAT FRACTION OF THE TOTAL REACH IS THE DISTANCE TO
 1 THE TERMINAL POINT?')
 85 READ(5,50)H
 90 FORMAT(F8.4)
 95 WRITE(6,55)
 100 FORMAT(' WHAT IS THE DIRECTION OF THE VELOCITY VECTOR?')
 105 READ(5,60)BETA
 110 FORMAT(F6.5)

115 DETERMINE THE ORTHOSIS ANGLES, PHI AND PSI

120 PHI=ACOS(((R**2.)*(1.+R)**2.)/((R**2.)+1.)) / ((-R.)*R.)
 125 PSI=PI-GAMMA+ACOS(((R**2.)*(1.+R)**2.)/(1.-(R**2.)))
 130 / ((2.*R*(1.+R)))

135 DETERMINE THE NORMALIZED ANGULAR VELOCITIES, DNPHI AND DNPSI

140 DNPHI=(H*(1.+R)*(COS(GAMMA)+(SIN(GAMMA)*TAN(BETA))))
 145 / (R*SIN(PHI))
 150 DNPSI=((R*(1.+R))/((R**2.)+1.-(2.*R*COS(PHI))))*
 155 ((SIN(GAMMA)-COS(GAMMA)*TAN(BETA))-((COS(GAMMA)+
 160 (SIN(GAMMA)*TAN(BETA)))*(R-COS(PHI)))/(SIN(PHI))))

165 DETERMINE THE X AND Y COMPONENTS OF THE NORMALIZED FORCE,
 C FXN AND FYN.

170 FXN=((R*COS((PHI+PSI))*B+DNPSI)/((COS((PI-PSI))+R*COS
 175 ((PHI+PSI))))*DNPHI)/(R*SIN((PI-PHI)))
 180 FYN=(((-R)*SIN((PHI+PSI))*B+DNPSI)/((SIN((PI-PSI))-
 185 (R*SIN((PHI+PSI))))*DNPHI)/(R*SIN((PI-PHI)))

C FOR THE PURPOSES OF PLOTTING, LET THE TOTAL REACH OF THE RESTRAINT
C EQUAL ONE DIMENSIONLESS UNIT, SO THAT THE DISTANCE TO THE TERMINAL
C POINT EQUALS P UNITS. USING THIS ASSUMPTION, THE COORDINATES OF THE
C TERMINAL POINT CAN BE DETERMINED W/RESPECT TO THE DEFINED UNITS

Y2=P+COS(GAMMA)
Y2=P*SIN(GAMMA)

C DEFINE THE POINTS TO WHICH THE COMPONENT FORCE VECTORS WILL BE
C DRAWN, SO THAT THE VECTORS WILL FIT ON THE PLOT, DIVIDE FXN AND
C FYN BY 20.

XF=X2+FXN/20.
YF=Y2+FYN/20.

C CALL THE SUBROUTINES WHICH WILL DRAW THE VECTORS

CALL MOVE(X2,Y2)
CALL DRAW(X2,YF)
CALL MOVE(X2,Y2)
CALL DRAW(XF,Y2)

C CHECK TO SEE IF ANY MORE PLOTS ARE DESIRED

100 WRITE(6,100)
1 FORMAT(' DO YOU WISH TO CHANGE ANY PARAMETERS AND OBTAIN MORE
1 PLOTS?IF YES,TYPE 1;IF NO, TYPE 0')
READ(5,105)REPLY

115 FORMAT(I1)
IF(REPLY.EQ.1) GO TO 5
CONTINUE

210 WRITE(6,200)
1 FORMAT(' DO YOU WISH TO OBTAIN MORE PLOTS WITH THE SAME PARAMETERS
1 IF YES, TYPE 1; IF NO,TYPE 0')
READ(5,205)ANSW

205 FORMAT(I1)
IF(ANSW.EQ.1) GO TO 30
END

C THIS PROGRAM IS DESIGNED TO COMPUTE THE RELATIVE MAGNITUDES OF THE
 C X AND Y COMPONENTS OF A NORMALIZED FORCE AT THE TERMINAL POINT ON
 C A VISCOUSLY DAMPED ARM RESTRAINT, GIVEN THE LOCATION OF THE TERMINAL
 C POINT, THE DIRECTION OF THE DAMPED VELOCITY VECTOR, AND THE RATIOS FOR
 C THE RESTRAINT LINK LENGTHS AND DAMPERS. THIS VERSION IS ADAPTED TO
 C ALLOW THE PROXIMAL LINK TO BE SHORTER THAN THE DISTAL LINK
 C

 SUBROUTINE FORCES
 INTEGER REPLY, ANSW
 PI=3.14159

C SPECIFY THE RATIOS OF THE CONTROLLING PARAMETERS, R AND B

 WRITE(6,10)
 10 FORMAT(' WHAT IS THE SIZE RATIO OF THE LINKS?')
 READ(5,15)R
 15 FORMAT(F8.4)
 WRITE(6,20)
 20 FORMAT(' WHAT IS THE DAMPER RATIO?')
 READ(5,25)B
 25 FORMAT(F8.4)

C SPECIFY THE INDEPENDENT VARIABLES, GAMMA, T, AND BETA

 WRITE(6,35)
 35 FORMAT(' WHAT IS THE DIRECTION OF THE TERMINAL POINT?')
 READ(5,40)GAMMA
 40 FORMAT(F9.5)
 WRITE(6,45)
 45 FORMAT(' WHAT FRACTION OF THE TOTAL REACH IS THE DISTANCE TO
 1 THE TERMINAL POINT?')
 READ(5,50)P
 50 FORMAT(F8.4)
 WRITE(6,55)
 55 FORMAT(' WHAT IS THE DIRECTION OF THE VELOCITY VECTOR?')
 READ(5,60)BETA
 60 FORMAT(F8.5)

C DETERMINE THE ORTHOGONAL ANGLES, PHI AND PSI

 PHI=ACOS(((R**2.)*((1.+P)**2.)-((R**2.)+1.))/((-2.)*P))
 PSI=PHI-GAMMA+ACOS(((R**2.)*((1.+P)**2.)+(R**2.-1.))
 1 /(2.*P*R*(1.+P)))

C DETERMINE THE NORMALIZED ANGULAR VELOCITIES, DPHI AND DPSI

 DPHI=(P*(1.+P)*(COS(GAMMA)+(SIN(GAMMA)*TAN(BETA))))
 1 /(R*SIN(PHI))

 DPSI=((P*(1.+P))/((R**2.)+1.-(2.*R*COS(PHI))))*
 1 ((SIN(GAMMA)-(COS(GAMMA)*TAN(BETA)))-((COS(GAMMA)+
 2 (SIN(GAMMA)*TAN(BETA))-(1.-R*COS(PHI)))/(R*SIN(PHI))))

C DETERMINE THE X AND Y COMPONENTS OF THE NORMALIZED FORCE,
 C FXN AND FYN

 FXN=(COS(PHI+PSI)*R*DPHI)-((R*COS(PHI-PSI)+(COS
 1 (PHI+PSI)))*DPHI)/(R*SIN(PHI-PSI))

 FYN=((-1.)*SIN(PHI+PSI)*R*DPHI)-((R*SIN(PHI-PSI)-
 1 (SIN(PHI+PSI)))*DPHI)/(R*SIN(PHI-PSI))

C
C FOR THE PURPOSES OF PLOTTING, LET THE TOTAL REACH OF THE RESTRAINT
C EQUAL ONE DIMENSIONLESS UNIT, SO THAT THE DISTANCE TO THE TERMINAL
C POINT EQUALS P UNITS. USING THIS ASSUMPTION, THE COORDINATES OF THE
C TERMINAL POINT CAN BE DETERMINED W/RESPECT TO THE DEFINED UNITS
C

X2=P*COS(GAMMA)
Y2=P*SIN(GAMMA)

C
C DEFINE THE POINTS TO WHICH THE COMPONENT FORCE VECTORS WILL BE
C DRAWN, SO THAT THE VECTORS WILL FIT ON THE PLOT. DIVIDE FXN AND
C FYN BY 20.
C

XF=X2+FXN/20.
YF=Y2+FYN/20.

C
C CALL THE SUBROUTINES WHICH WILL DRAW THE VECTORS
C

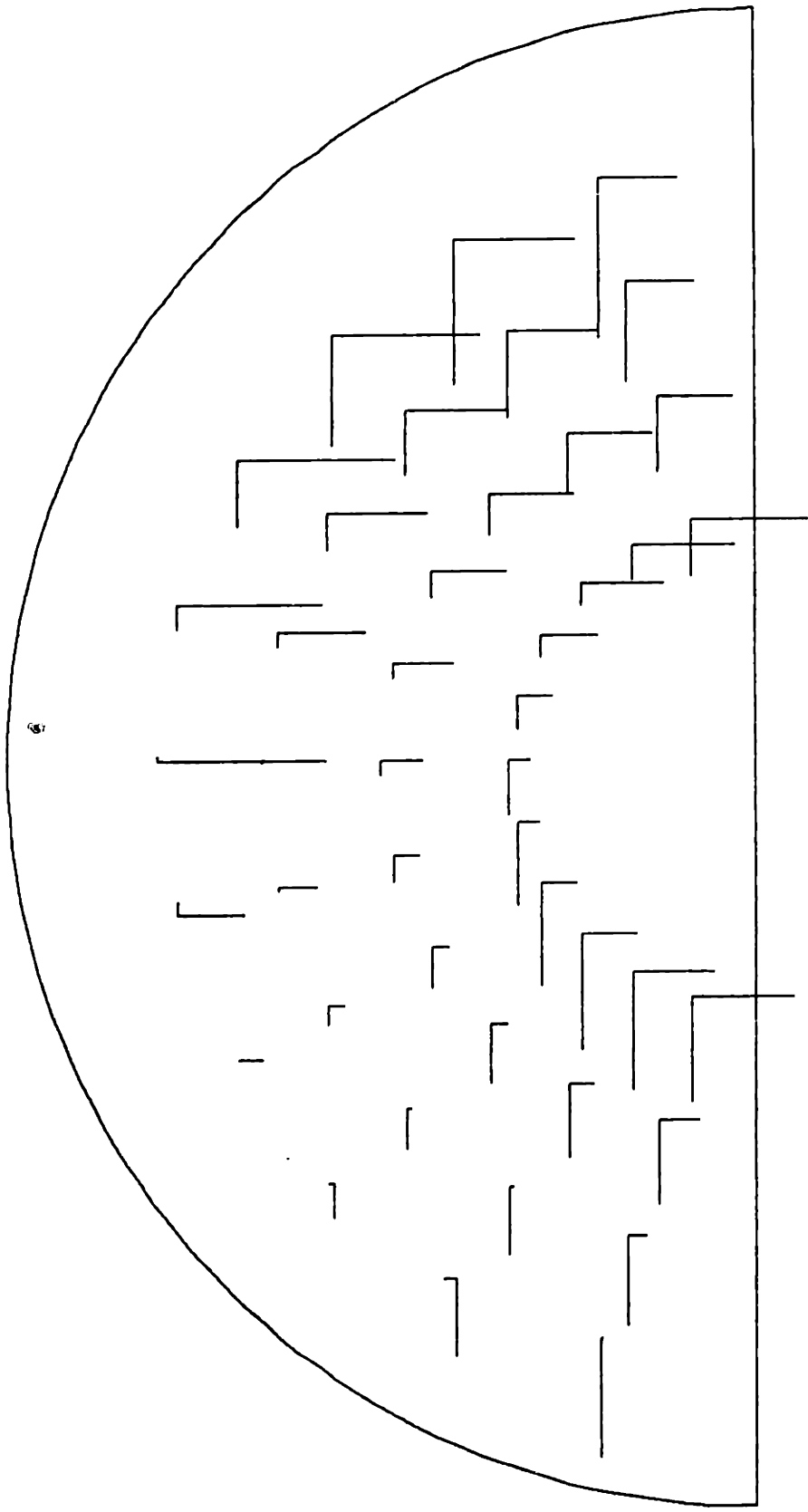
CALL MOVE(X2,Y2)
CALL DRAW(X2,YF)
CALL MOVE(X2,Y2)
CALL DRAW(XF,Y2)

C
C CHECK TO SEE IF ANY MORE PLOTS ARE DESIRED
C

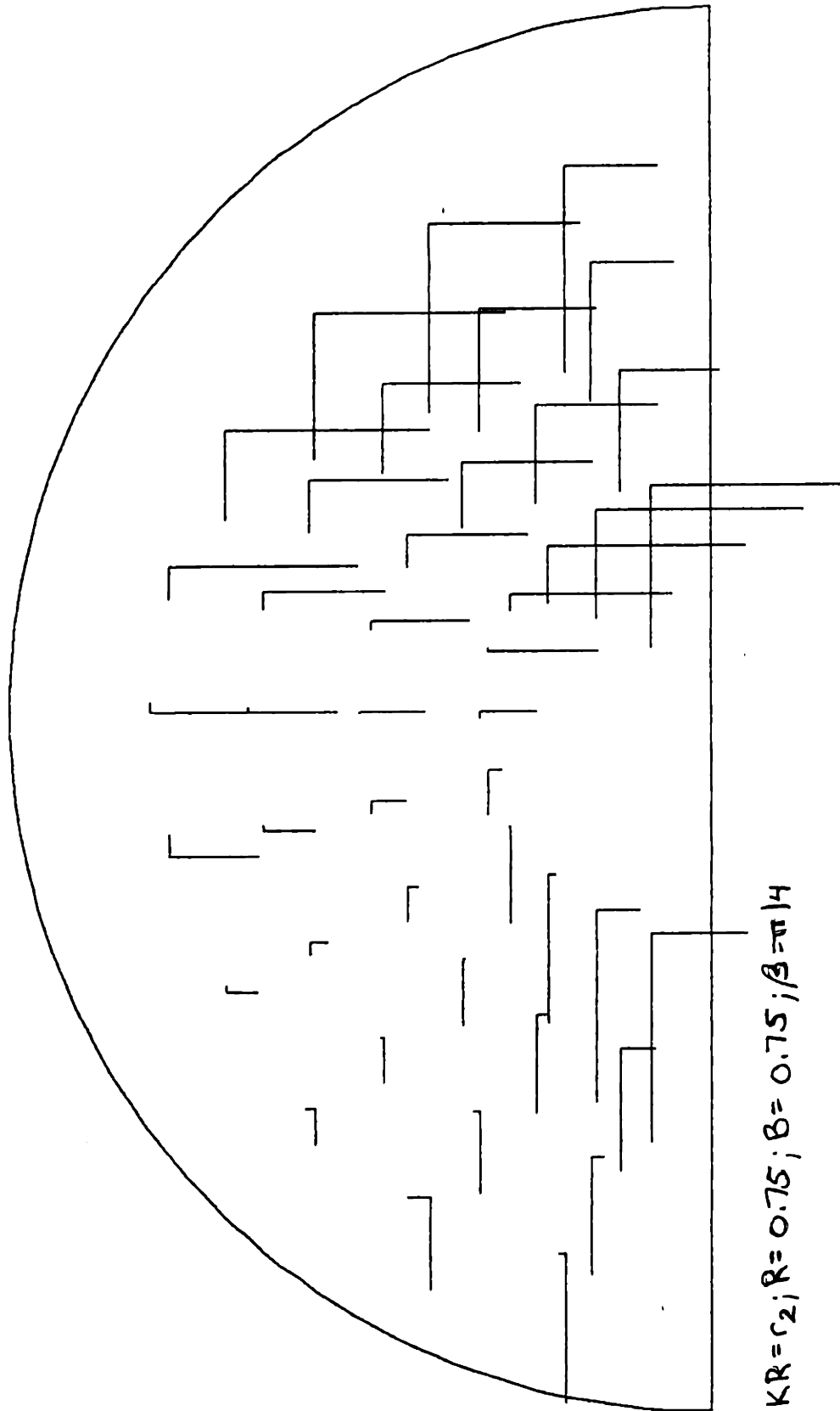
100 WRITE(6,100)
1 FORMAT(' DO YOU WISH TO CHANGE ANY PARAMETERS AND OBTAIN MORE
1 PLOTS? IF YES, TYPE 1; IF NO, TYPE 0')
105 READ(5,105)REPLY
106 FORMAT(I1)
107 IF(REPLY.EQ.1) GO TO 5
108 CONTINUE
200 WRITE(6,200)
201 FORMAT(' DO YOU WISH TO OBTAIN MORE PLOTS WITH THE SAME PARAMETER
1 IF YES, TYPE 1; IF NO, TYPE 0')
202 READ(5,202)ANSW
203 FORMAT(I1)
204 IF(ANSW.EQ.1) GO TO 31
205 END

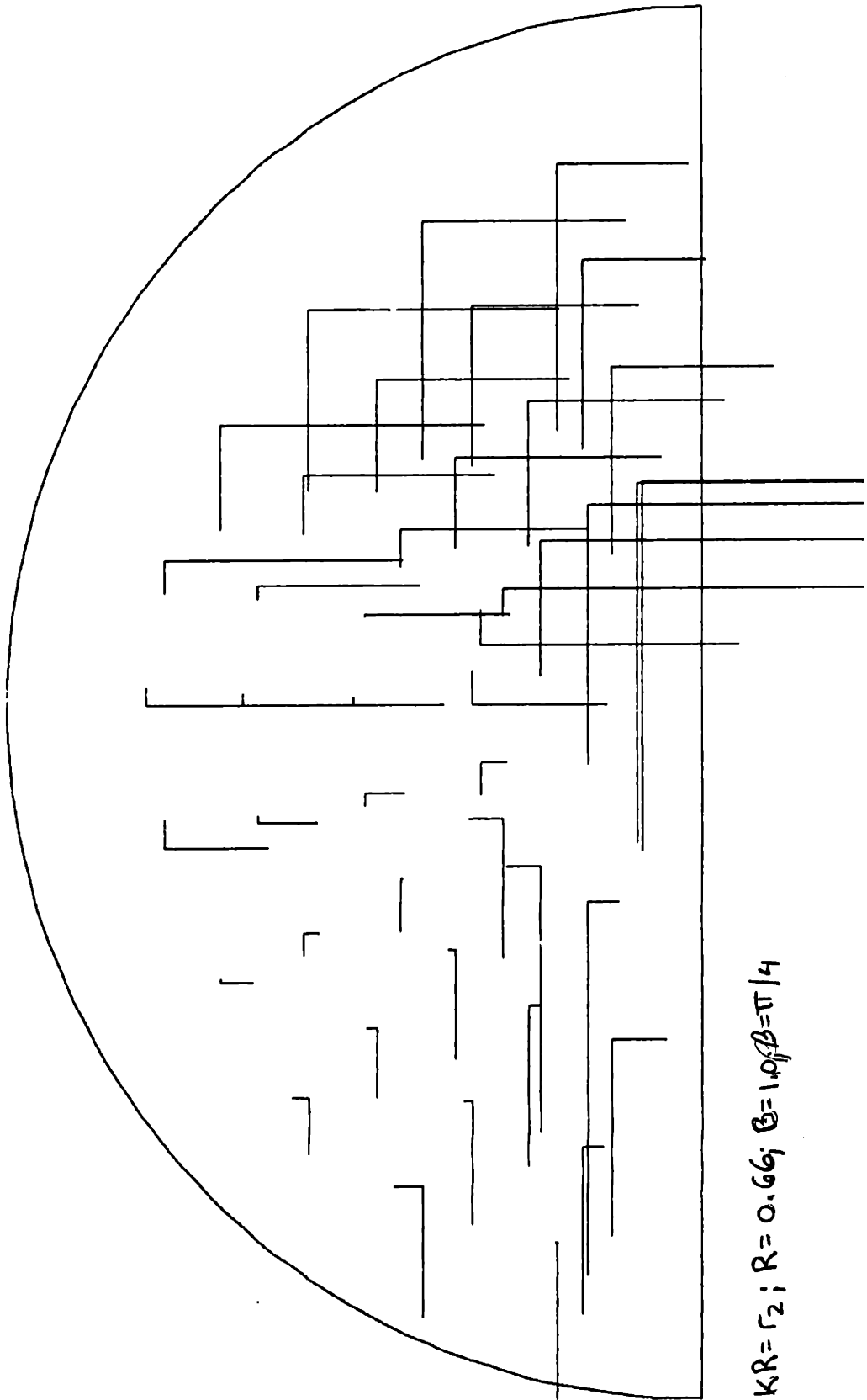
Appendix B

Plots of Normalized Force Components

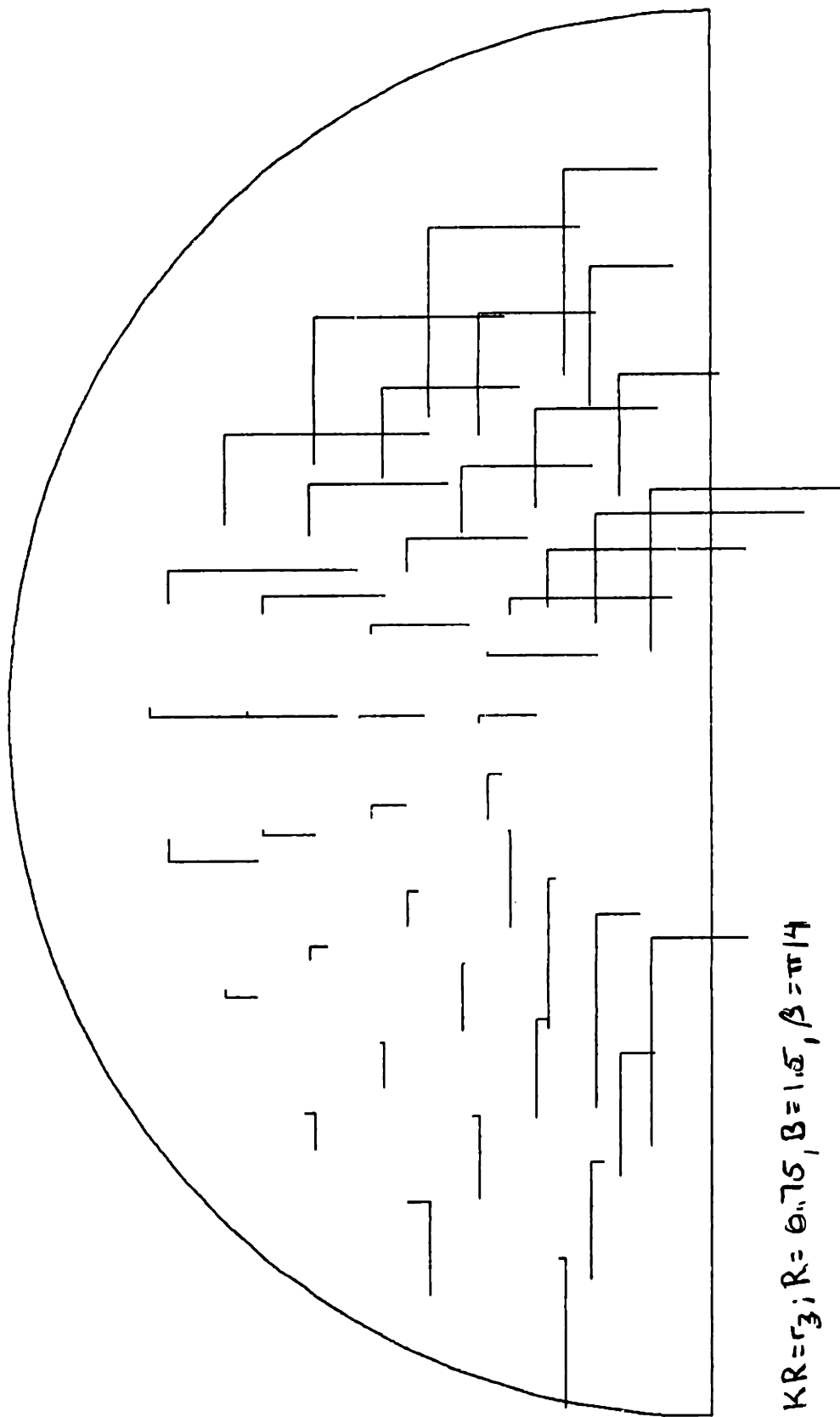


$KR = \sqrt{2}$; $R = 1.0$; $B = 1.0$; $\beta = \pi/4$

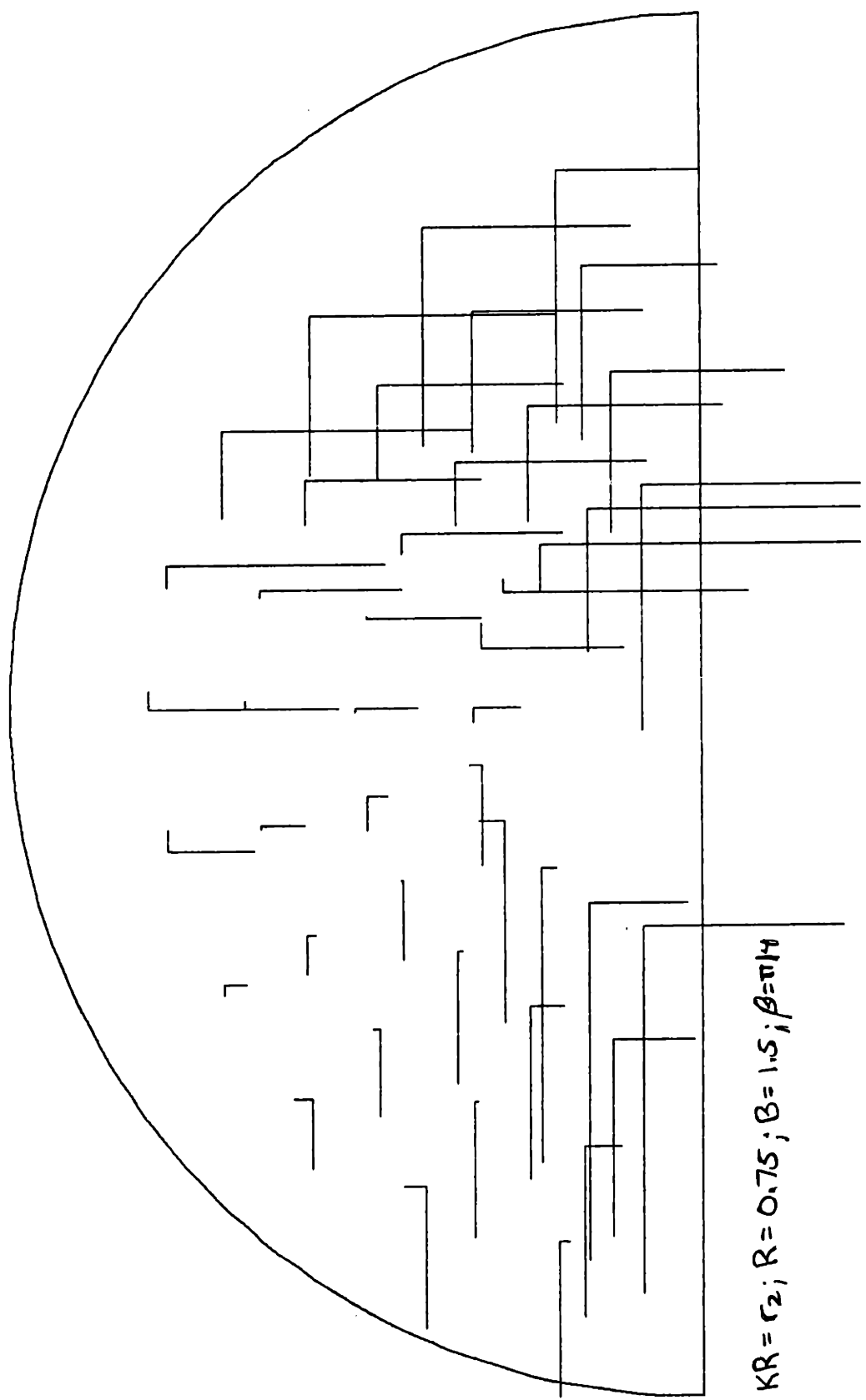




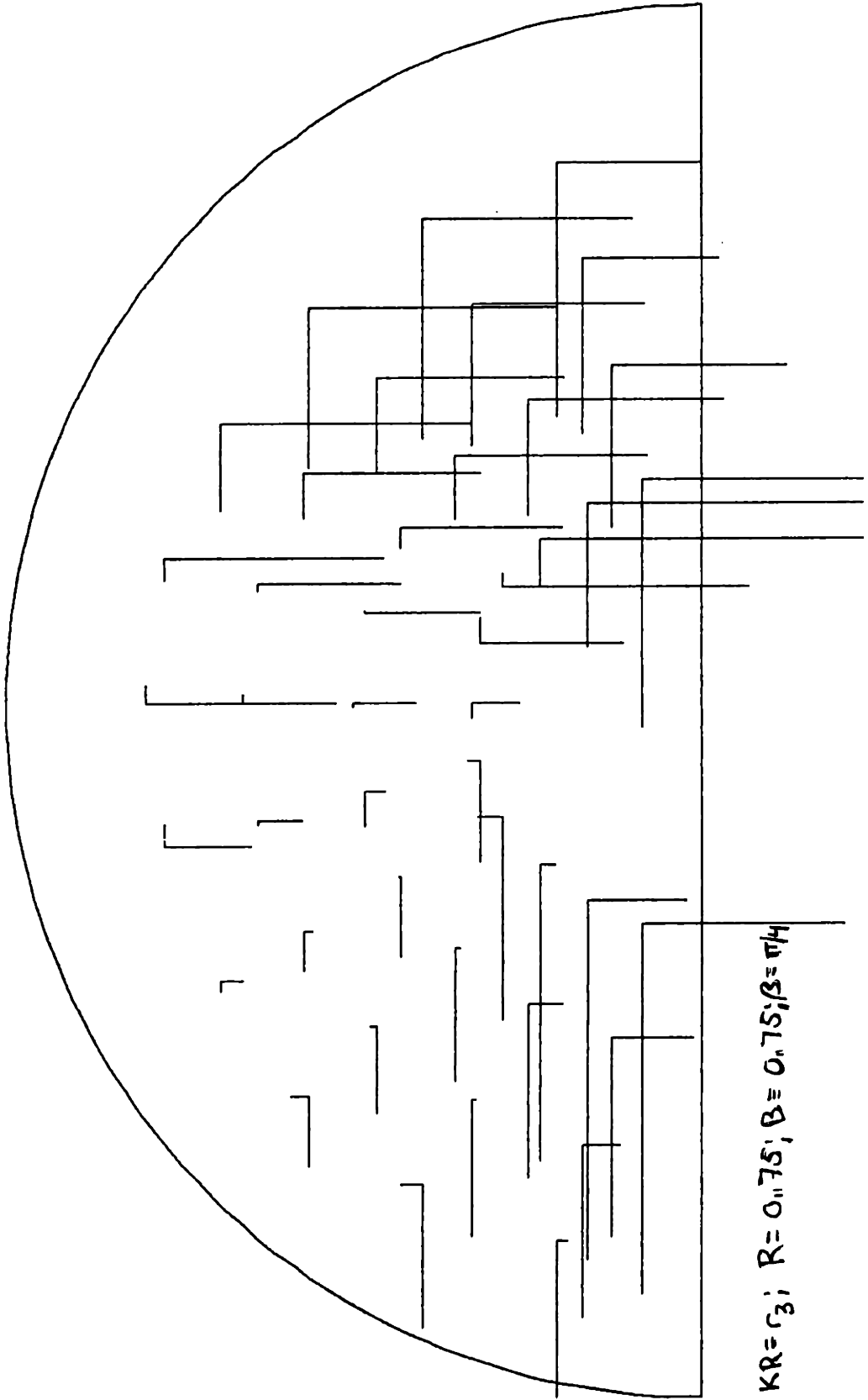
$KR = r_2$; $R = 0.66$; $B = 1.0$; $\beta = \pi/4$



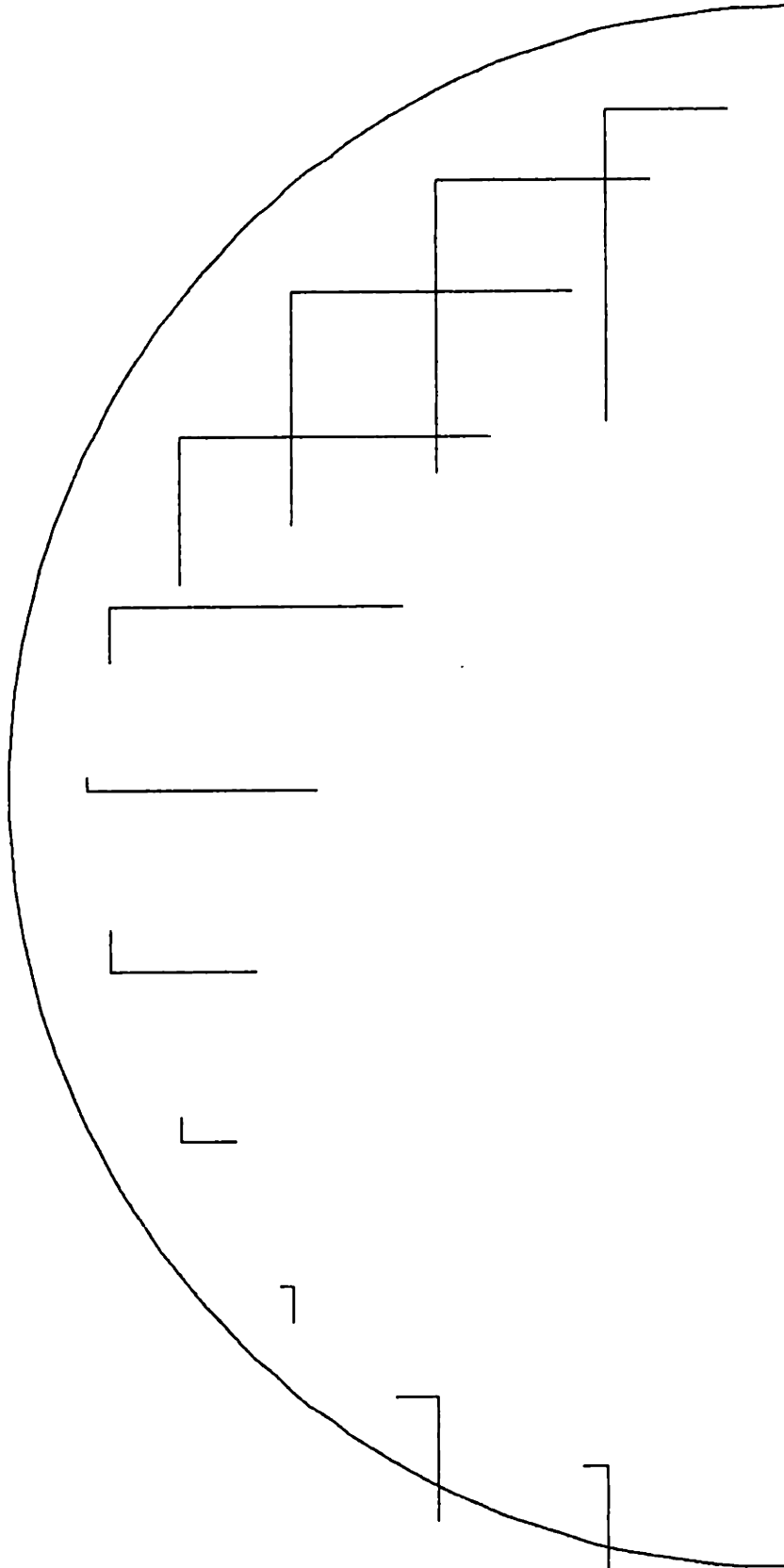
$KR = r_3; R = 0.75, B = 1.5, \beta = \pi/4$



$KR = r_2; R = 0.75; B = 1.5; \beta = \pi/4$



$KR = \zeta_3; R = 0.75; B = 0.75; \beta = \pi/4$



$R=1, \beta=1, P=0.9, \theta=\pi/4$

REFERENCES

1. Chusid, J.G.: Correlative Neuroanatomy and Functional Neurology. (Lange, Los Altos, CA. 1979)
2. Fee, James W., Jr.: "The Design and Building of a Writing Machine." Proceedings, 1972 Carnahan Conference on Electronic Prosthetics, University of Kentucky, Lexington, Kentucky, Dec. 1972, Patent No. 3, 864, 515, February 4, 1975.
3. Horn, Berthold K.P.: "Kinematics, Statics, and Dynamics of Two-D Manipulators". Massachusetts Institute of Technology, Artificial Intelligence Laboratory, Working Paper 99, June 1975.
4. Joyce, G.C. and Rack, P.M.H.: "The effects of load and force on tremor at the normal human elbow joint." J. Physiol., London, 240: 375-396 (1974).
5. Morgan, M.H., Hewer, R.L., Cooper, R.: Application of an Objective Method of Assessing Intention Tremor-A Further Study on the Use of Weights to Reduce Intention Tremor. J. of Neurology, Neurosurgery, and Psychiatry 38: 259-264, 1975.
6. Preston Corporation: Special Education Catalogue, 1981.
7. Rondet, P.; Jedynack, C.P. and Ferrey, G.: Pathological Tremors: no sological correlates; in Physiological Tremor, Pathological Tremors and Clonus. Prog. Clin. Neurophysiol., vol.5, ed. J.E. Desmedt, pp. 114-128 (Karger, Basel 1978)
8. Rosen, M.J.: Suppression of pathological tremor by application of viscous damping. Proceedings, 4th Ann. New England Bioeng. Conf., New Haven, May 1976.
9. Rosen, M.J., Biber, C.R.: Attenuation of Abnormal Intention Tremor Following Viscous Exercise: Work in Progress. Proceedings, International Conference on Rehabilitation Engineering, Toronto, 1980.
10. Rosen, M.J., Sloan, M.H., Biber, C.R.: A Damped Joystick: Adaptive Control for the Tremor Disabled, Proceedings, 2nd Interagency Conference on Rehabilitation Engineering, Atlanta, August 1979.
11. Shahani, B.T. and Young R.R.: Action Tremors: a clinical neurophysiological review; in Physiological Tremor, Pathological Tremors and Clonus. Pro. Clin. Neurophysiol. vol. 5, ed. J.E. Desmedt, pp. 129-137 (Karger, Basel 1978)